Phytoliths (Plant-Derived Mineral Bodies) as Geobiological and Climatic Indicators in Arid Environments

K. DAISY MORGAN-EDEL[1,2], PENELOPE J. BOSTON[1,2], MICHAEL N. SPILDE[3], and ROBERT E. REYNOLDS[4]
[1]Earth & Environmental Sciences Dept., New Mexico Institute of Mining & Technology, Socorro, New Mexico, 87801; [2]National Cave & Karst Research Institute, Carlsbad, New Mexico, 88222; [3]Institute of Meteoritics, University of New Mexico, Albuquerque, New Mexico, 87131; [4]Redlands, California 92373.

Abstract

Phytoliths are plant-derived mineral bodies. They have been used in a variety of archaeological, environmental, and climate studies to infer paleoclimate from the vegetation types represented by diagnostic phytolith morphologies. Phytoliths can be recovered from modern plants, soils, sediments, lacustrine deposits, eolian deposits, archaeological sites, plant fossils, and potentially allochthonous sediment deposits in caves. In order to interpret such data, documentation of modern plant-derived minerals is needed, especially in arid regimes. Four goals were attempted in this study, 1) provide a morphological description of the different types of biomineralization products from the modern plant species of creosote and horsetail, two Southwestern plants with significantly different environmental requirements; 2) describe the elemental chemistry and mineralogy of the phytoliths from these plants; 3) describe morphological changes to biominerals during experimental mechanical weathering and abrasion processes, and; 4) compare all of these results to identified fragments of potential phytoliths and preserved plant-derived minerals from Fort Stanton Cave sediments and Miocene-aged plant fossils from the Rainbow Loop Flora of the Barstow Formation.

This study examines biominerals from two modern key indicator species in the arid Southwest U.S.A.: *Larrea tridentata* (DC.) Coville (creosote), which is characteristic of North American hot arid regimes, and *Equisetum hyemale* L. (horsetail), a known silica accumulating plant from wet environments and an indicator of riparian areas within desert environments. Creosote and horsetail produce biominerals that are different from one another, and possibly unique to the species or genus level of identification. We conducted a series of observations, analyses, and experiments including: 1) analysis of plant tissues with scanning electron microscopy (SEM) with energy dispersive x-ray (EDX) and x-ray diffraction (XRD); 2) investigation of preservation potential by documenting morphological changes to phytoliths after simulated mechanical weathering for different lengths of time; and 3) modern and weathered biominerals from creosote and horsetail were compared to sediments and fossils of different ages from two study sites, Fort Stanton Cave, Lincoln County, New Mexico and the Barstow Formation, San Bernardino County, California. Both study sites revealed preserved phytoliths indicating potential long-term preservation and the potential for application of these structures as vegetation paleoclimate indicators. All phytolith types from modern plant material were still distinguishable after simulated weathering treatments.

Introduction and Background

Plant-derived mineral bodies, known as phytoliths, can provide geological evidence of the presence of indicator plant species and therefore record the environmental conditions at the time of deposition. Phytolith records have been preserved in soils and sediments (Twiss et al. 1969; St. Clair and Rushforth 1976; Budel et al. 1993; Romero et al. 1999; Yost and Blinnikov 2011), and at archaeological sites, both in caves and surface environments (Kurmann 1985; Reinhard and Danielson 2005; Cabanes et al. 2009, 2010). Previously, pollen and other vegetation indicators from sediments and speleothems in caves have been used to infer surface vegetation types at the time of deposition (Brook et al. 1990; Carrión et al. 1999); these records have paleoclimate significance by reflecting ecological conditions on the surface at the time of cave flooding. To our knowledge, phytoliths have not been searched for in cave deposits, nor used in the context of paleoclimate and ecological interpretations.

The overarching hypothesis of this study is that plant biominerals can be preserved in cave and fossil deposits and be sufficiently identifiable to provide information about past surface vegetation that may be useful in interpreting the climate present during deposition. Predictions that flow from this hypothesis include: 1) key indicator species that are characteristic of specific environmental conditions possess phytoliths that may be unique to a species or genus level of identification, 2) phytoliths can retain diagnostic characteristics even after damage by weathering and transport, 3) such phytoliths can be recovered from deposits of sediment in caves and from the surface, and 4) phytoliths present in ancient plants may be left within the fossil imprints and detectable.

We systematically worked through the following steps. First, we examined two key indicator species for the presence of biominerals: *Larrea tridentata* (DC.) Coville (creosote bush) characteristic of North American hot arid regions and *Equisetum hyemale* L. (horsetail), a known silica (Si) accumulating plant found in wet environments. Secondly, we identified the mineral composition and documented phytolith morphologies for these two plants to understand what might be found in sedimentary deposits. Thirdly, to determine if phytoliths are still recognizable after weathering, we investigated aspects of preservability of these biominerals from creosote and horsetail focusing on morphological changes in simulated mechanical weathering experiments. Next, to test our prediction that phytoliths would actually be present in environments of interest, we also searched for biominerals in cave sediments from Fort. Stanton Cave (FSC), Lincoln County, New Mexico, and in rock samples from the Miocene-aged, fossiliferous Rainbow Loop Flora (RLF) of the Barstow Formation in the Mojave Desert, San Bernardino County, California. Finally, we compared the modern and weathered biomineral products of our studies to the FSC sediments and to the Miocene-aged plant fossils from the (RLF) in the Barstow Formation to test the prediction that we can recognize them in situ and draw conclusions about vegetation sources.

For the purpose of this study, the term "phytolith" will be used to describe all plant mineral bodies, regardless of their chemical composition. In some studies, distinctions have been made between opalline (amorphous) Si bodies, referring to them as "phytoliths" whereas all other chemical compositions of mineral bodies were referred to with other terms, such as crystaliths (Mulholland and Rapp, Jr. 1992; Prychid and Rudall 1999; Gobetz and Bozarth 2001; Madella et al. 2005; Piperno 2006; Borrelli et al. 2011).

Biomineralization

Biomineralization is ubiquitous in living organisms and occurs within all six classical kingdoms and the myriad of kingdoms within the Bacteria and Archaea (Skinner 2005). The definition of "biomineral" offered by Skinner (2005) is "*a subset of the*

mineral kingdom, created through the actions and activity of a life form." Mineral utilization and production are adaptive strategies used by living organisms to provide structure (Perry et al. 2007; Koch et al. 2009; Bauer et al. 2011), detoxify certain compounds (Prychid and Rudall 1999; Franceschi and Nakata 2005), and to excrete waste material from cellular processes (Franceschi and Nakata 2005). Many vascular plants appear to have mastered the art of biomineralization to provide mechanisms for coping with environmental stresses, including structural strength, mineralized stomata (gas exchange location), anti-grazing protection, and even as light scatterers to enhance photosynthetic light-harvesting or to reflect high intensity solar radiation in arid regimes (Franceschi and Nakata 2005; Reinhard and Danielson 2005; Piperno 2006; Perry et al. 2007; Koch et al. 2009; Gal et al. 2012).

Various members of the vascular plants are known to produce amorphous silica, calcium salts such as carbonates, oxalates, phosphates, and sulfates (Driessens and Verbeeck 1990), and other sulfates such as strontium (celestite) and barium (barite) (Raven and Giordano 2009). These materials are frequently precipitated as both amorphous and crystalline structures alongside cellulose, lignin, and other organic molecules (Piperno 2006). Phytoliths, or "plant stones" are found in the plant's leaves, stems, reproductive structures, and roots. They can be located in a number of internal places including inside of the cells, inside the plant's vacuoles, associated with vascular bundles, scattered in epidermal and parenchymatous tissue, in the leaf mesophyll, between palisade and spongy parenchyma, associated with aerenchyma tissue and also surrounding or within the stomata, lining the walls and other cell organelles, or they can even be precipitated extracellularly (Prychid and Rudall 1999; Monje and Baran 2004; Franceschi and Nakata 2005; Koch et al. 2009; Bauer et al. 2011; Borrelli et al. 2011). Frequently, plant mineralized epidermal tissue is observed in patterns given morphologically evocative names like wavy, jigsaw, square, rectangular, polyhedral, or favose honeycomb patterns (Piperno 2006). Thus, fossilized phytoliths can potentially reveal a great deal about cellular structure from different plant species.

Calcification seems to have arisen in plant lines very early on, and apparently evolved independently at least once in each of five different Classes within the plant kingdom: Florideophyceae (red algae), Ulvophyceae (a subset of the green algae), Charophyceae (green algae most closely related to vascular plants), Phaeophyceae (brown algae) and Prymnesiophyceae (an algal group that contains the coccolithophores) (Raven and Giordano 2009). Calcium-containing phytoliths are often called crystal sand, cystoliths, druses, raphides, or crystal idioblasts (Mulholland and Rapp, Jr. 1992; Prychid and Rudall 1999; Addadi et al. 2003; Monje and Baran 2004; Franceschi and Nakata 2005; Raven and Giordano 2009; Bauer et al. 2011).

Interestingly, many plants produce a suite of phytoliths of many mineral compositions. Biogenic amorphous calcium carbonate (ACC) has been found in conjunction with significant quantities of magnesium and/or phosphorous minerals, and those secondary elements have been hypothesized to function in formation and/or the stabilization of mineral phases (Addadi et al. 2003). Additionally, calcite has been found within plant cystoliths in species like mulberry (*Morus alba*), where the calcite crystals in mature leaves are surrounded by a siliceous sheath (Bauer et al. 2011).

One form of calcic mineral, crystalline calcium oxalate, is the most widespread biomineralization product across the plant kingdom (Bauer et al. 2011). Frequently, the crystalline idioblasts are made up of two calcium oxalate minerals, weddellite and whewellite (Prychid and Rudall 1999; Frost and Weier 2003, 2004; Monje and Baran 2004; Franceschi and Nakata 2005; Bauer et al. 2011). Garvie (2003) showed in saguaro cacti (*Carnegiea gigantia*), that the initial mineral weddellite manufactured by the plant is derived from atmospheric CO_2 via photosynthesis. Then upon plant death, the weddellite is subjected to a complex series of mineral transformations during the various stages of decay, undoubtedly assisted by microbial processes. The minerals produced include authigenic Mg- and Ca-bearing minerals including lansfordite ($MgCO_3S_5H_2O$), nesquehonite ($MgCO_3S_3H_2O$), several polymorphs of $MgC_2O_4S_2H_2O$ including glushinskite, monohydrocalcite ($CaCO_3SH_2O$), calcite, vaterite, magnesium oxalates, and several other unidentified Mg-bearing phases. In the iconic saguaro cacti, the atmospheric CO_2 is ultimately altered from weddellite to calcite, which serves as a net long-term sink of carbon into soils where this particular cactus is abundant (Garvie 2003).

Interestingly, silica-based plant biominerals are most often amorphous (opalline) silica structures, in contrast to the calcareous crystalline minerals such as calcite, whewellite and weddellite mentioned above (Prychid and Rudall 1999; Frost and Weier 2003, 2004; Monje and Baran 2004; Franceschi and Nakata 2005; Bauer et al. 2011). Silica phytoliths with unique identifiable characters can be used to identify specimens to family, genus, and sometimes species level. They are produced in large quantities by many plants; however not all plant groups produce silicate biominerals (Twiss et al, 1969; Kurmann 1985; Piperno 2006; Yost and Blinnikov 2011). For example, no siliceous phytoliths have been documented in the Araceae, Amaranthaceae, Chenopodiaceae, and Cactaceae families (Piperno 2006). In contrast, grasses possess the highest morphological diversity of silica phytoliths, and have been used to infer ecological changes in the landscape (Twiss et al., 1969; Kurmann 1985; Piperno 2006). In addition, their phytoliths have been studied more than other plant species. Serious investigative phytolith research in areas of taphonomy, ecology, climate and archaeological applications did not start until the late 1970s and early 1980s (Twiss et al. 1969; Brooks et al. 1981; Brook et al., 1990; Reinhard and Danielson 2005; Piperno 2006), so this is still a developing field. Whereas silica-derived bodies have been used in many applications, analyses of calcic plant-derived bodies have not been widely applied in archaeological and paleoecological research.

Several different phytolith morphologies and chemistries can exist within the same plant and examples of some diverse morphologies with both silica and calcium from plants in our collection can be seen in Fig. 1. These mineral bodies vary significantly in size, with a range of 1–500 micron diameters.

Water, Weathering, and Transport

Despite the low amount of annual precipitation characteristic of arid environments, water plays a critical role in weathering and transport of materials, even in these dry situations. Channels created from heavy monsoonal precipitation and episodic flooding can dominate the desert landscape. Ephemeral pools and streams are formed as a byproduct of intermittent precipitation events. Riparian zones are narrow strips of terrain immediately adjacent to the banks of both perennial and ephemeral watercourses. They are exceptions to the general aridity of desert regions and can be short-lived potentially because of seasonal drying, alteration in drainage locations, stream piracy, and other geomorphic and hydrologic changes. Such zones are frequently characterized by horsetails on stream banks and in marshy areas, and tree species such as cottonwoods, poplars, and willows, but have also been subjected to the human introduction of non-native tree species including salt cedar (*Tamarix ramosissima*) and Russian olive (*Elaeagnus angustifolia*), which have negatively impacted the native trees (Dick-Peddie 1993; Granados-Sánchez et al. 2011). All of these manifestations of water show that significant aqueous weathering and transport via moving water are important processes in arid environments.

Phytolith production is a geobiological process dependent on both biotic and abiotic factors, such as physical environmental conditions, soil, hydrology, and genetics (Twiss 1992; Piperno 2006). Phytoliths are released into the environment through vegetative decay, fire, and herbivore consumption and deposition (Piperno 2006; Andrews et al. 2008; Cabanes et al 2011). Then these microfossils can be transported by wind, water, animals, fire, and geological processes, such as volcanic events and

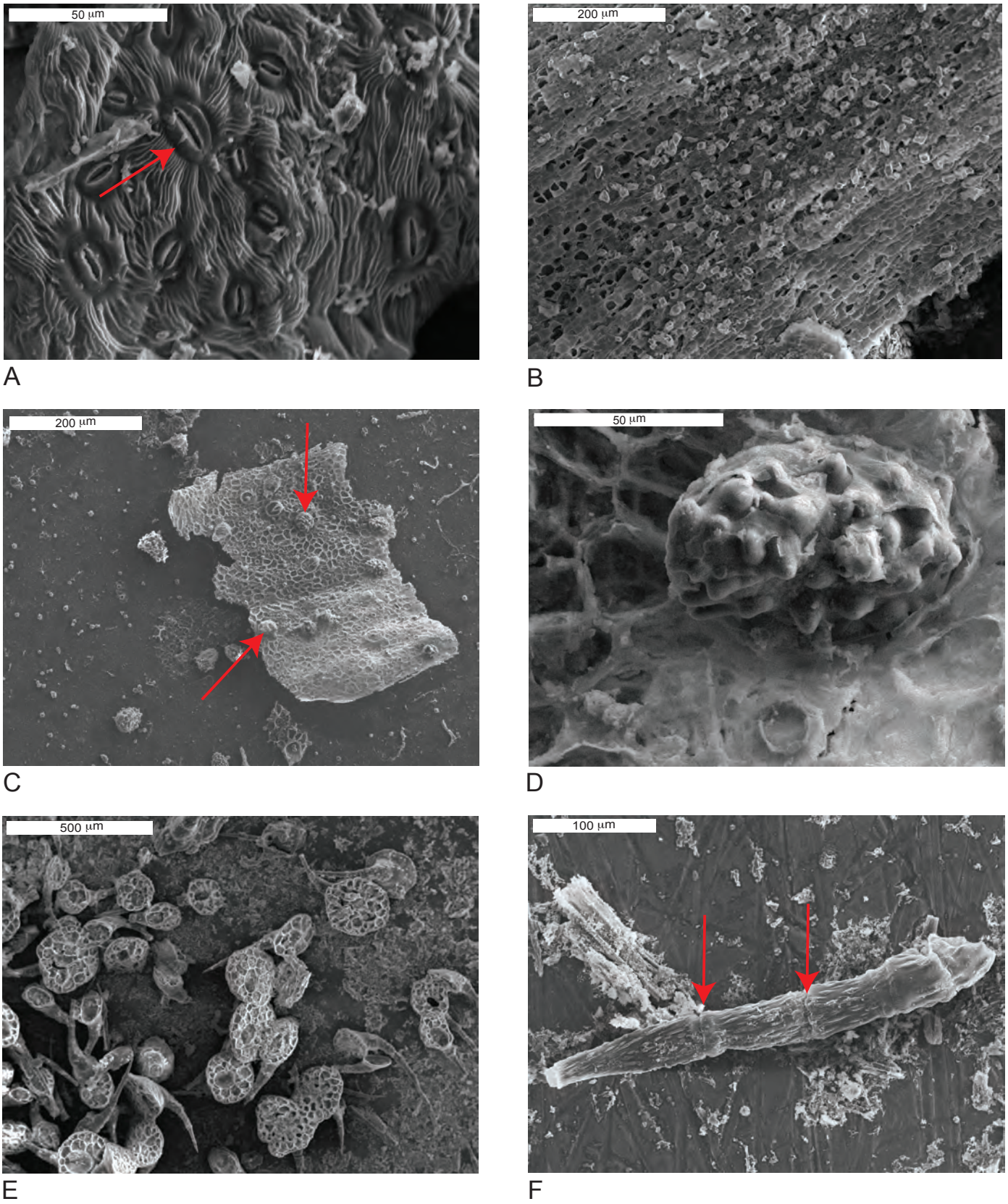

Figure 1—Overview comparison of selected phytolith morphologies from our larger modern plant collection. **A)** *Morus alba* (mulberry) leaf showing a mass of stomata (red arrow) amidst crenellated tissues, all of silica composition. **B)** Mulberry twig showing cubic phytoliths of calcic composition against silicified tissue. **C)** *Ficus benjamina* (weeping fig) leaf tissue reveals a silicified favose epidermis with calcic globular echinate (rosette) crystals in situ (red arrows). **D)** Weeping fig high magnification of rosette crystals. **E)** *Helianthus maximiliani* (Maximilian's sunflower) leaf tissue shows the abrasive hairs on the surface of the leaf are silicified and resemble pointy hats, called hair cells and hair cell bases (Madella et al. 2005). **F)** High magnification of an individual hair cell reveals a striated surface texture that is segmented (red arrows indicate segment joints).

landslides (Romero et al. 1999; Piperno 2006; Andrews et al. 2008; Channing et al. 2011).

The geomorphology and hydrological patterns dictate sediment transport within systems. Flooding events are agents of erosion, sedimentation, and transport of materials, sometimes into karstic areas including caves (Granados-Sánchez et al. 2011; Land 2012). Without an extensive vegetation cover that protects the land and halts the descent of water down the slope, the amount of washout transported to the rivers is often very large (Granados-Sánchez et al. 2011). Large air masses can also transport particles over large distances. Phytoliths and diatoms have been found to travel great distances in Saharan dust clouds, even passing over the Atlantic Ocean (Romero et al. 1999). The amount of diatoms captured by the air sediment traps in that study ranged from just 100 to 15,000 valves per day, while the phytolith numbers ranged from just a few to 20,000 mineral bodies per day in the same amount of material.

Regional Southwestern Deserts

The North American deserts present a spectrum of conditions that partially overlap, but also have significant and distinctive individual properties that are reflected in the types of vegetation present. For example, the arid regions of the Mojave, Sonoran, and Chihuahuan deserts are considered to be hot deserts, while the Great Basin Desert is a cooler environment, and this is reflected in plant communities and endemic plant species such as Lechuguilla in the Chihuahuan Desert (Granados-Sánchez et al. 2011). Each desert has different geomorphologies, precipitation patterns, and vegetative ecologies that are distinct from one another, yet there are also transitory ecotones between some desert boundaries, and some plant species such as creosote can survive in multiple deserts (Baldwin 2002; Dodson 2012).

Chihuahuan Desert Characteristics

The Chihuahuan Desert is the second largest desert in North America and extends from south-central New Mexico at the northern boundary, south into Mexico into the San Luis Potosi region, with small eastern outliers in Texas and western parts in Arizona (Granados-Sánchez et al. 2011). The northern Chihuahuan Desert is a sensitive climate zone where shifts in atmospheric circulation greatly affect the amount and distribution of rainfall (Van Devender et al. 1984). The region has many diverse plant communities as determined by Granados-Sánchez et al. (2011), which partially overlap 13 different vegetation zones described in New Mexico (Dick-Peddie 1993), but also includes some additional communities and some that are not represented. Granados-Sánchez et al. (2011) divided the Chihuahuan Desert into these regions based on vegetation composition and soil types: 1) *Larrea tridentata* (creosote) microphyll desert scrub linked with alluvial soils, 2) *Agave lechuguilla* (lechuguilla), *Dasylirion* spp. (sotols) and Yucca sp. (many common names) rosette desert scrub linked with limestone areas and well-drained soils, 3) crassicaule scrub (*Opuntia* sp. dominated) linked with igneous soils, 4) Grama-dominated grassland, 5) desert grassland, 6) chaparral (submontane oak dominated at higher elevations than grasslands), 7) mesquite, 8) dune vegetation, 9) gypsum soils with gypsophilic plant inhabitants, 10) halophytic vegetation (salt tolerant), 11) piñon-juniper woodlands, 12) coniferous forests, 13) fir forests, and 14) riparian vegetation. We have chosen two species from these myriad communities as key indicators of shifts in climate boundaries, namely *Larrea tridentata* microphyll desert scrub and riparian vegetation represented by the iconic horsetails.

Plants: *Larrea tridentata and Equisetum hyemale*

The two modern plant species, *Larrea tridentata* and *Equisetum hyemale* (Fig. 2), were selected for their contrasting habitats and environmental conditions (arid and riparian), and their contrast in mineralogy (calcic and siliceous). Both occur in the southwestern United States, but reflect distinct moisture, slope, and altitude niches. These plants' ecological importance is also reflected in their use by ancient peoples in the region and this provides additional insight into their distribution (Bowers 1993; Reinhard and Danielson 2005; Dodson 2012).

Larrea tridentata (common names: creosote, creosotebush, and greasewood) is an evergreen desert shrub dominant in all three hot North American deserts (Dodson 2012). It forms clonal colonies, and the most ancient one in North America is 12,000 years old and located in the Mojave Desert (Vasek 1980). Categorized as belonging to the Family Zygophyllaceae Caltrop, creosote has many-branched stems up to 2 meters or more in height. The plants have small compound leaves with 5–10 mm long oblong to obovate leaflets, small yellow flowers from April to June or longer, and fruit about 5 mm in diameter covered in dense white hairs (Martin and Hutchins 1980). Creosote is a strongly scented resinous shrub well known to perfume the air across broad distances during rainstorms. It prefers dry mesas and alluvial fans at altitudes of 3,000–5,000 ft (910–1525m).

The *Larrea tridentata* microphyll desert scrub is characterized by the dominance of small-leaved shrub species in addition to creosote, some thorny and some not, and by succulent, ephemeral plants that grow on alluvial fans, plains, bajadas, valleys, and gentle hills. This community is located mainly in the valleys, where soils are fine-textured, deep to relatively deep, and have a layer of rocks (Granados-Sánchez et al. 2011). In the modern New Mexico landscape, *Larrea tridentata* can be seen growing in some of the hottest and driest places in the state where the shrubs are quite stunted in height and yet still abundant and flowering.

Although creosote has been classified in the past as a non-producer of phytoliths (using the exclusively silica-based definition, Piperno 2006), it has been shown to take up metal ions including copper from the soil (Gardea-Torresdey et al. 1997, 2001). Thus, the capability clearly exists for this species to manipulate geochemical compounds from the environment. An additional line of evidence of creosote's potential ability to take up and manipulate minerals, may be seen in the use of herbal infusions of creosote which can dissolve calcium oxalate calculi from human organs such as the kidney, gallbladder and urinary bladder (Pinales et al. 2010).

Equisetum hyemale (common names: scouring rush, horsetail) is a riparian indicator species in the arid west with greater distribution beyond just the riparian zone in wetter climates; hence it is dependent on reliable moisture. It is a perennial plant, with all stems identical in structure, typically erect and unbranched up to a meter or more in height (Martin and Hutchins 1980). Horsetail is widespread along riparian areas at 5,000–8,000 ft (1,525–2,450 m) in New Mexico and can even invade moist areas of residential gardens throughout the state. It is classified within the Equisetales, an order of the Pteridophytes, that includes vascular plants that use spores for reproduction and dispersal, and originated about 358 million years ago during the Carboniferous. *Equisetum* is the only remaining extant genus consisting of about 30 species (Channing et al. 2011). Whisk ferns and horsetails were once classified as "Fern Allies" but are now classified along with ferns (Smith et al. 2006).

It appears that ability to take up silica and metals probably is of great antiquity in this group. Horsetail species are capable of taking up gold (Au), tellurium (Te), zinc (Zn), copper (Cu), silver (Ag), chromium (Cr), arsenic (As), antimony (Sb), and lithium (Li) from the environment (Brooks et al. 1981; Florea et al. 2008). Silica uptake and deposition has been postulated to have evolved early on in terrestrial plant evolution and is important to plant functions such as mechanical stability of tissues, protection against predation and pathogens, light reflection, and resistance to drought through controlled water loss (Chauhan et al. 2009; Yamanaka et al. 2012). Horsetail is well known for high production of phytoliths and mineralized tissues, which have taxonomic significance

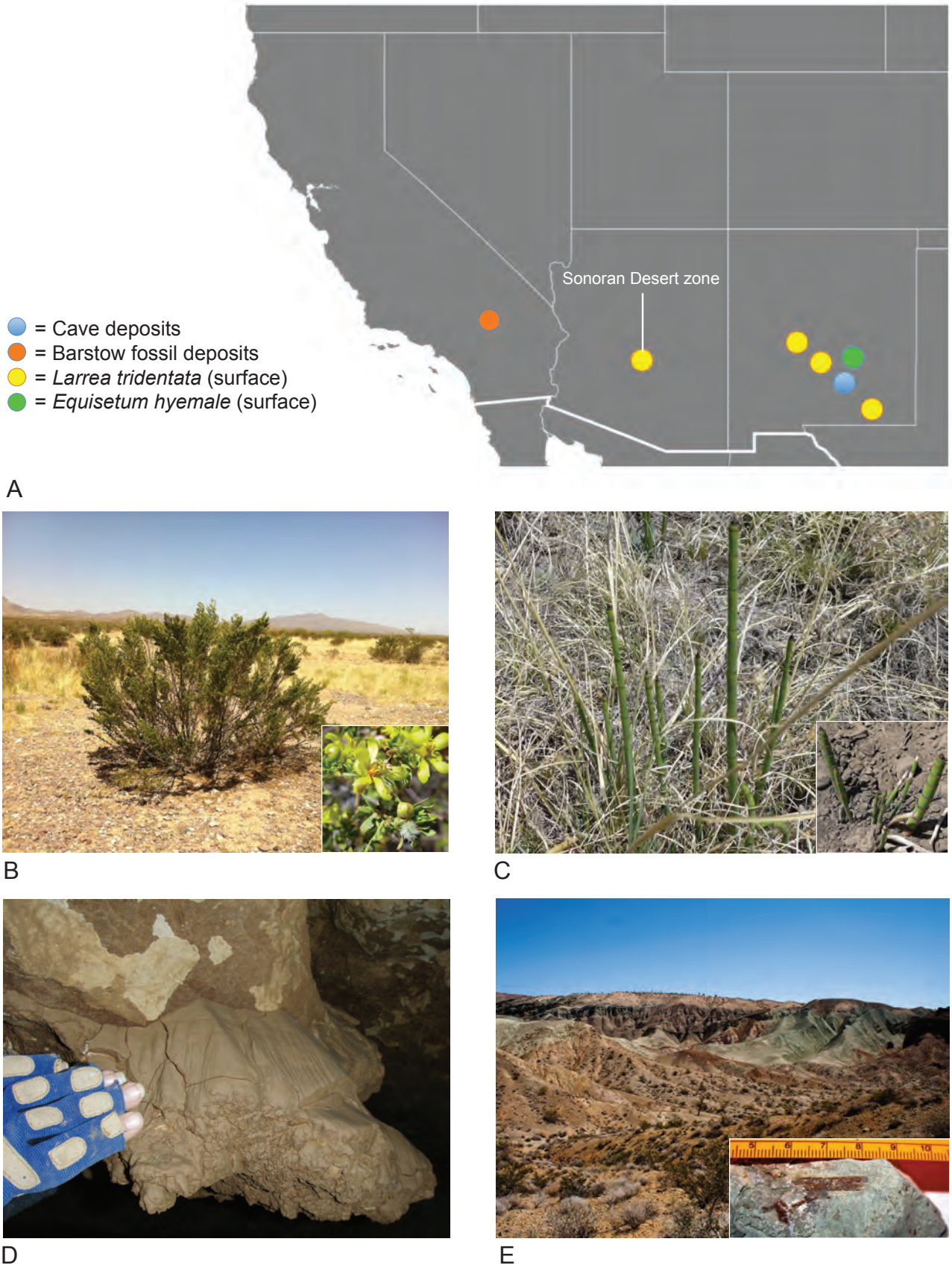

Figure 2—**A)** Sample location map. **B)** *Larrea tridentata* (creosote shrub), which grows in the Chihuahuan, Sonoran, and Mojave deserts and was sampled at several locations within the Chihuahuan Desert and one sampling location within the Sonoran desert; insert is inflorescence. **C)** *Equisetum hyemale* (horsetail) growing in a dense stand along the banks of the Rio Bonito, Lincoln County, NM, insert shows reproductive sporangia. **D)** Mud Mushroom formations in Fort Stanton Cave, Lincoln County, NM. Samples in this study were taken from these flow-deposited features that accumulate on prominences that extend from the limestone bedrock. **E)** Overview of the fossiliferous Miocene Barstow Formation, near Barstow, San Bernardino County, CA, insert of rock material with plant fossils. Fossil plant remains (about 2 cm in length) were examined for this study.

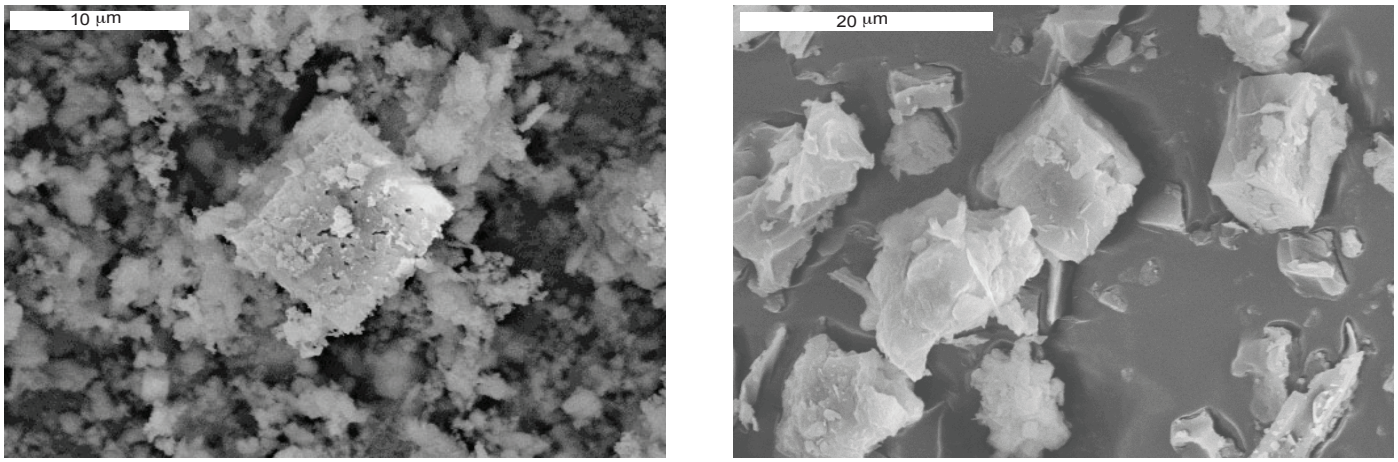

A B

Figure 3—High temperature ashing procedures (above 600°C) appear to dehydrate and degrade the physical structure of cubic and parallelepipedal (rhombohedral) calcium oxalate phytoliths, due to a phase change from weddellite to whewellite at temperatures over 420°C (Frost and Weier 2003: 2004). **A)** This image shows an example of a creosote crystal that was ashed at a temperature range of 450–620°C exhibiting a friable texture with small holes visible on the crystal faces. Possible dehydration and decarbonation (i.e. loss of carbon as CO_2) is the most likely chemical consequence. **B)** This image shows the typical appearance of calcic phytoliths ashed at lower temperatures (390°C) where the crystal faces seem unaffected by heating. These results encouraged us to develop methods that utilized lower temperature preparation.

(Brooks et al. 1981; Piperno 2006; Neumann et al. 2010; Law and Exley 2011; Mazumdar et al. 2011; Yamanaka et al. 2012). Piperno (2006) characterized Equisetaceae as contributing large stomatal and epidermal phytoliths with either smooth (psilate) or grainy (granulate) surfaces.

The Field Region around Fort Stanton Cave (FSC)

There are several agencies involved with the management of the land in the region. The Capitan Mountains have a Wilderness Area designation and are managed by the USDA Forest Service (USFS). The Sacramento Mountains Escarpment is an Area of Critical Ecological Concern managed by the Bureau of Land Management (BLM). Fort Stanton Cave is one of the sixteen areas in the National Landscape Conservation System (NLCS) designed to protect and preserve unique historical, cultural, and scientific important areas within the US (Land 2012). The cave is managed by the BLM and is also an Area of Critical Ecological Concern (Dick-Peddie 1993).

In the mountainous regions, the major floristic communities (approximately in order of increasing elevation with overlap in some areas) are piñon-juniper forests, mixed conifer woodlands and montane coniferous forest, subalpine coniferous forests, spruce-fir forests, montane grasslands (mountain meadows), alpine-tundra zones, and alpine and montane riparian areas (Martin and Hutchins 1980; Dick-Peddie 1993). The mountains are surrounded by lower elevation Chihuahuan Desert, juniper savanna (transitional ecotone), desert and Plains-Mesa grassland communities, and riparian areas. Ocotillo is known to grow preferentially on limestone ridge areas (Martin and Hutchins 1980; Dick-Peddie 1993).

The field region in and around FSC (Fig. 2) is located within the Upper Rio Hondo Watershed, which has a northern border of the Capitan Mountains, a western boundary of the Sacramento Mountains, a southern boundary of the Pajarita Mountains and an eastern drainage into the Pecos River. The watershed has an elevation differential of 8558 feet (2608 m) from high to low points. The headwaters of the Rio Bonito start in the Sacramento Mountains and eventually join up with the Rio Ruidoso and both drain into the Rio Hondo (Weisner et al. 2004). The Rio Bonito separates the igneous Sacramento Mountains from the Capitan Mountains batholiths to the north and FSC lies within the Permian San Andres limestone at the northern end of the Sacramento Mountains (Land 2012). As of late 2014, it is the second longest cave in New Mexico at more than 43 km in length and contains the longest continuous calcite speleothem on the planet, the Snowy River Formation, whose exploration is ongoing and currently maps at more than 18 km (Land 2012; Fort Stanton Cave Study Project, unpublished data, 2014).

Stream flow into FSC and onto the Snowy River formation seems to be from different sources, since Snowy River is not always flooded at the same time as the main cave passages. Flow in Snowy River runs from south to north, and at the northern end discharges into Government Spring, which drains into the Rio Bonito (Land 2012). Cave water sources could be from the Rio Bonito, sinking streams, subterranean pools, or the base level water table. Land (2012) speculates that the presence of water on the Snowy River formation is correlated with extreme precipitation events in the Sacramento Mountains, either due to heavy summer monsoons or heavy winter snowmelt.

The Barstow Formation field site

The Barstow Formation in the Mojave Desert, San Bernardino County, California (Fig. 2) is a series of lacustrine limestones, conglomerates, sandstones, siltstones and shales of Middle Miocene age (Dibblee 1967). The rock units contain several areas of identified fossil beds. The Rainbow Loop Flora (RLF) in the Mud Hills area has at least 13 terrestrial plant taxa that have been identified including juniper, oak, ash, and mountain mahogany. Additionally, the presence of sedges and cattail are the first indication of a wet period in this area in the Miocene (Reynolds and Schweich 2013). These fossils have been found in a Brown Platy Limestone (BLP) sequence below a Strontium-Borate horizon, and have been magnetostratigraphically dated between 16.4-16.2 Ma.

Methods

Plant Sampling

Creosote leaflets and branches were collected at several locations: in the Chihuahuan Desert in Socorro County, near the New Mexico Tech campus, near the Blanchard Mine (Lincoln County, NM), near Sitting Bull Falls (Eddy County, NM), and in the Sonoran Desert outside of Phoenix, AZ (Fig. 2A and 2B). Plant samples were prepared in slightly different ways: all were rinsed with distilled water and dried in an oven at 90°C; the

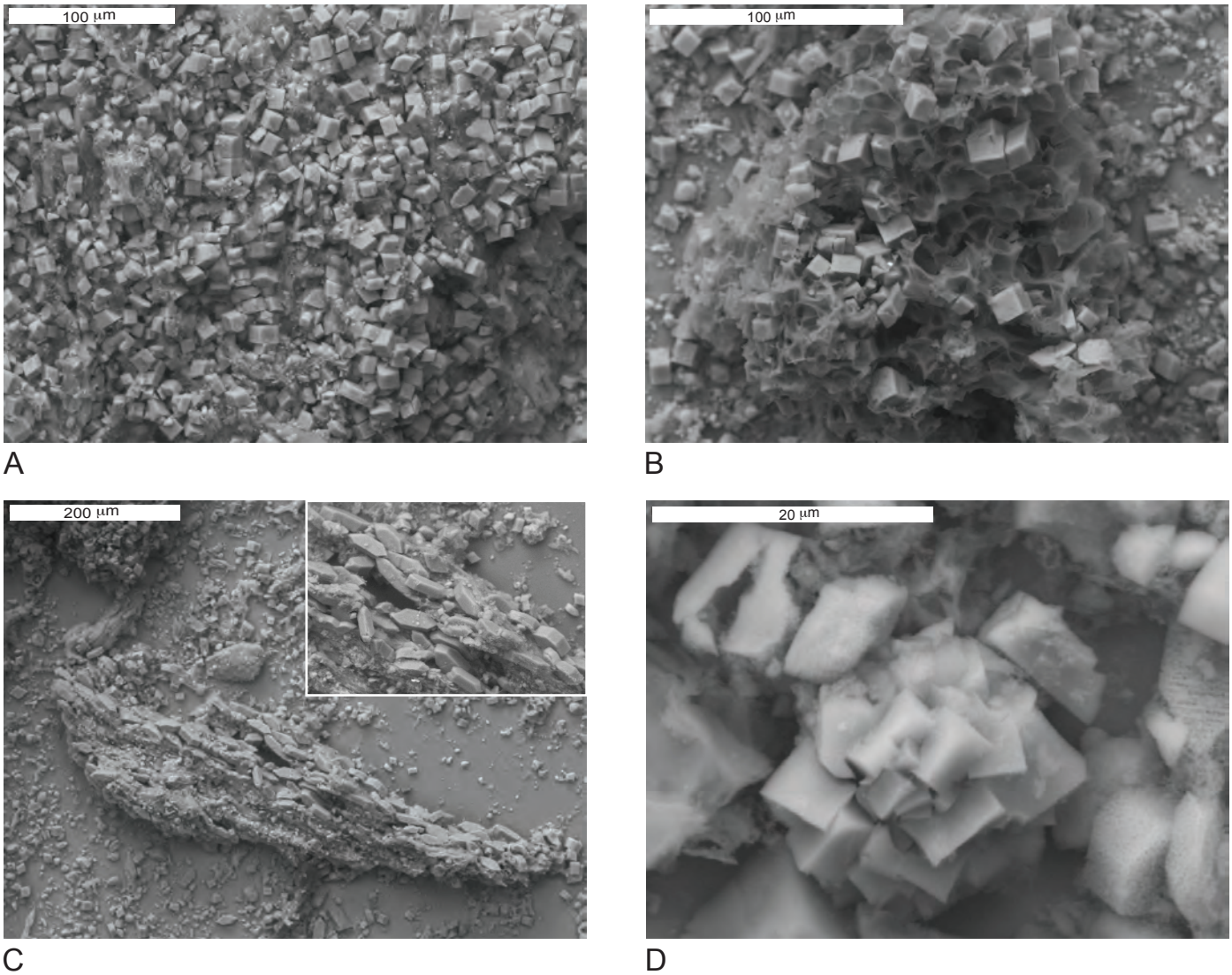

Figure 4—Phytolith morphologies of calcic-rich creosote wood (*Larrea tridentata*) from Phoenix, AZ. **A)** Overview of hundreds of cubic, parallelepipedal (rhombohedral), and tabular oblong phytolith morphologies. **B)** Cubic minerals in situ and empty cells within a segment of incompletely ashed cellular tissue. **C)** Tabular oblong calcic phytoliths in situ within a tissue fragment. Enlarged insert shows monoclinic crystal morphologies lineated within the tissue. **D)** Interpenetrating twins of calcic blocks forming a globular echinate (rosette) shape.

Chihuahuan Bingham Mine District specimens (Fig. 3) were collected first and dry ashed in a muffle furnace at 450–620°C for 3 hours; the Sonoran specimens were dry ashed at 360°C for 17.5 hours; and the Socorro samples were ashed at 390°C for 28.5 hours.

Live horsetails were collected along the banks of the Rio Bonito drainage west of FSC, part of the Upper Hondo Watershed (Fig. 2A and 2C). Plant material was washed with distilled water, dried at 90°C, then dry ashed in a muffle furnace at 580°C for 2 hours.

Living Plant Phytolith Separation

There are several published protocols available to liberate phytoliths from modern plants including acid digestion, dry ashing, and microwave techniques (Parr et al. 2001; Parr 2002; Piperno 2006; Katz et al., 2010; Cabanes et al. 2011; Yost and Blinnikov 2011). We chose to use the dry ashing method and modified it to account for all potential phytolith chemistries, as many methods are used primarily for silica biominerals. Standard dry ashing protocols recommend ashing at 450–550°C for different time lengths (Parr et al 2001; Piperno 2006; Cabanes et al. 2011; Mazumdar 2011; Yost and Blinnikov 2011). We ultimately lowered our ashing temperature in an attempt to avoid excessive dewatering or mineral phase changes with high temperatures (Fig. 3).

Our initial temperature constraints were determined from the phytolith methodology literature (Piperno 2006; Mazumdar 2011; Yost and Blinnikov 2011). However, our final temperature selections were based on the mineralogy literature. For example, in a study of the calcium oxalate dihydrate mineral, weddellite (Frost and Weier 2003), it was determined that this mineral undergoes three mass loss steps at increasing temperatures. The first step is a dehydration reaction at 97°C that results in a conversion into monohydrate calcium oxalate (whewellite) and then another mineral change into anhydrous calcium oxalate at temperatures above 114°C. Next, at temperatures above 422°C, there is loss of carbon monoxides and dioxides, and a mineral conversion into calcium carbonate (calcite). Lastly, the mineral totally degrades at temperatures above 650°C. Additionally, Frost and Weier (2004) found that the calcium oxalate monohydrate mineral, whewellite, also undergoes three mass loss steps as it is heated; these temperatures are slightly hotter than for weddellite. In the first step, water is lost at temperatures above 161°C; next, carbon monoxide and dioxide is lost at temperatures greater than 459.1°C, resulting in a mineral change into calcium

Plant	Plant Part	Phytolith Type	Associated Figure
Creosote	Leaf	Globular echinate	6A, 8A
		Cubic	6A
		Parallelepipedal	6A
Creosote	Wood	Globular echinate	4D, 7A
		Cubic	4A, 4B, 6B, 7A, 9A
		Parallelepipedal	4A, 4B, 4C, 6B, 9A
		Tabular oblong	4A, 4C, 6B, 7A, 9A, 9B
		Pyramidal	7A
Horsetail	Stem and leaf	Elongate echinate long-cells	5C inset, 7B
		Cylindrical polylobate	5C-D, 6C
		Acicular (needle-like)	5B, 5C, 6C, 7B
		Papillate and crenulated epidermal tissue	5A, 5C, 7B
		Stomata	5A, 5B, 5D, 6C, 7B, 8C
		Stomata comb	5B, 5D, 6C, 8C
Mulberry	Leaf	Stomata	1A
		Crenulated tissue	1A
	Twig	Cubic	1B
Weeping Fig	Leaf	Favose epidermis	1C
		Globular echinate	1C-D
Maximilian's Sunflower	Leaf	Hair cells	1E-F

Table 1—shows phytolith morphologies represented in each plant and gives their corresponding Figures for easy reference.

carbonate. Finally, at temperatures higher than 684°C, calcium oxide is formed. This is important in understanding mineral identification and potential dehydration and mineral changes that can take place during dry ashing of the samples (Fig. 3). Cabanes et al. (2011) also found that heating silica phytoliths above 500°C increased their overall solubility due to dehydration effects. We have attempted to use the lowest possible temperatures to combust the live plant material without altering the mineral contents (Fig. 3).

Cave Sediment and Fossil Sampling

Sediments were collected from passages in FSC (Fig. 2D). Samples were examined after three types of treatment: 1) no processing; 2) after agitation with sodium hexametaphosphate solution followed by separation into sand, silt, and clay fractions (Day 1965); and 3) after heavy liquid separation using sodium polytungstate (SPT) adjusted to a specific gravity of 2.3 (Piperno 2006).

Rock samples with visible plant fossil fragments were collected from the Miocene-aged RLF from the Mud Hills section of the Barstow Formation (Fig. 2E). Fossil imprints were identified and cut into smaller pieces, in preparation for scanning electron microscopy examination.

Scanning Electron Microscopy (SEM)

Samples were examined using SEM for potential plant-derived mineral bodies. We used the International Code for Phytolith Naming (Madella et al. 2005) to describe all morphological features for potential chemical compositions. Ashed plant material and sediment sample analysis was carried out on a JEOL JSM5800LV scanning electron microscope in the Department of Earth and Planetary Sciences/Institute of Meteoritics, University of New Mexico. The SEM is equipped with both secondary electron (SE) and backscattered electron (BSE) imaging detectors. The SE image provides topographical information about the surface of the sample, whereas the BSE image provides spatial chemical information; in the BSE image, higher atomic number materials appear brighter and lower atomic number material, darker. Geological samples and some ashed samples were coated with an evaporated film of gold-palladium alloy to make them conductive under the electron beam. The samples were analyzed with a range of accelerating voltages up to 20 kV.

The SEM is a "low vacuum" microscope that can operate at both high vacuum (the conventional mode of operation) and in a low or poor vacuum, to 100 Pa. We used low vacuum mode to enable imaging and analysis of uncoated and "wet" samples in an attempt to preserve the original spatial relationships of phytoliths to each other and to the original tissue matrix. Low vacuum mode was used to analyze uncoated plant samples to obtain optimized morphological images. The samples were analyzed with an accelerating voltage of 20 kV and a chamber vacuum of 31 Pa. The SEM is also equipped with an Oxford Instruments Energy Dispersive X-ray spectrometer (EDX) and an Oxford X-ray analyzer.

X-Ray Diffraction (XRD)

The mineralogical content of the samples was determined by X-Ray diffraction (XRD) analysis at the New Mexico Bureau of Geology and Mineral Resources, Socorro, NM. Samples were ground with a ceramic mortar and pestle to a particle size of approximately 20 micrometers. A small amount of the powdered sample was placed on an indented silicon wafer and pressed to uniform height before analysis in a Panalytical X'Pert Pro powder diffractometer. Mineral spectra were collected from 6 to 70° 2-Theta with a wide-angle high-speed detector that facilitates rapid data acquisition; each spectrum was accumulated for 20 minutes. Semi-quantitative phase analysis was done using the Reference Intensity Ratio method included with the Panalytical High Score Plus software (PANalyical B.V., Almelo, Netherlands).

Mechanical Weathering Simulation Experiments

Plant tissues can be subjected to compressive mechanical weathering through mastication by teeth or physical grinding by humans. Additionally, decaying plant tissues and liberated biomineral products can be physically weathered during hydrological and eolian transport. This simulation experiment was meant to mimic some of these processes by grinding the ash material with coarse sand using a mortar and pestle for differing time intervals.

A small amount of modern plant ash was mixed with Ottawa sand (Fisher Scientific) in equal parts by volume, and wetted with a small amount of distilled water. The sample was manually ground with a small mortar and pestle for five different time steps, 5, 30, 60, 120, and 300 seconds. A sampling of ash and sand mixture was taken at each time step. All samples were put on a glass slide, vacuum dried at a low temperature, left uncoated, and examined with the SEM using the low vacuum mode.

Results

There are four specific tasks completed in this study: 1) development of a morphological description of the different types of biomineralization products from the modern plant species of creosote and horsetail, two Southwestern plants with significantly different environmental requirements; 2) a description of

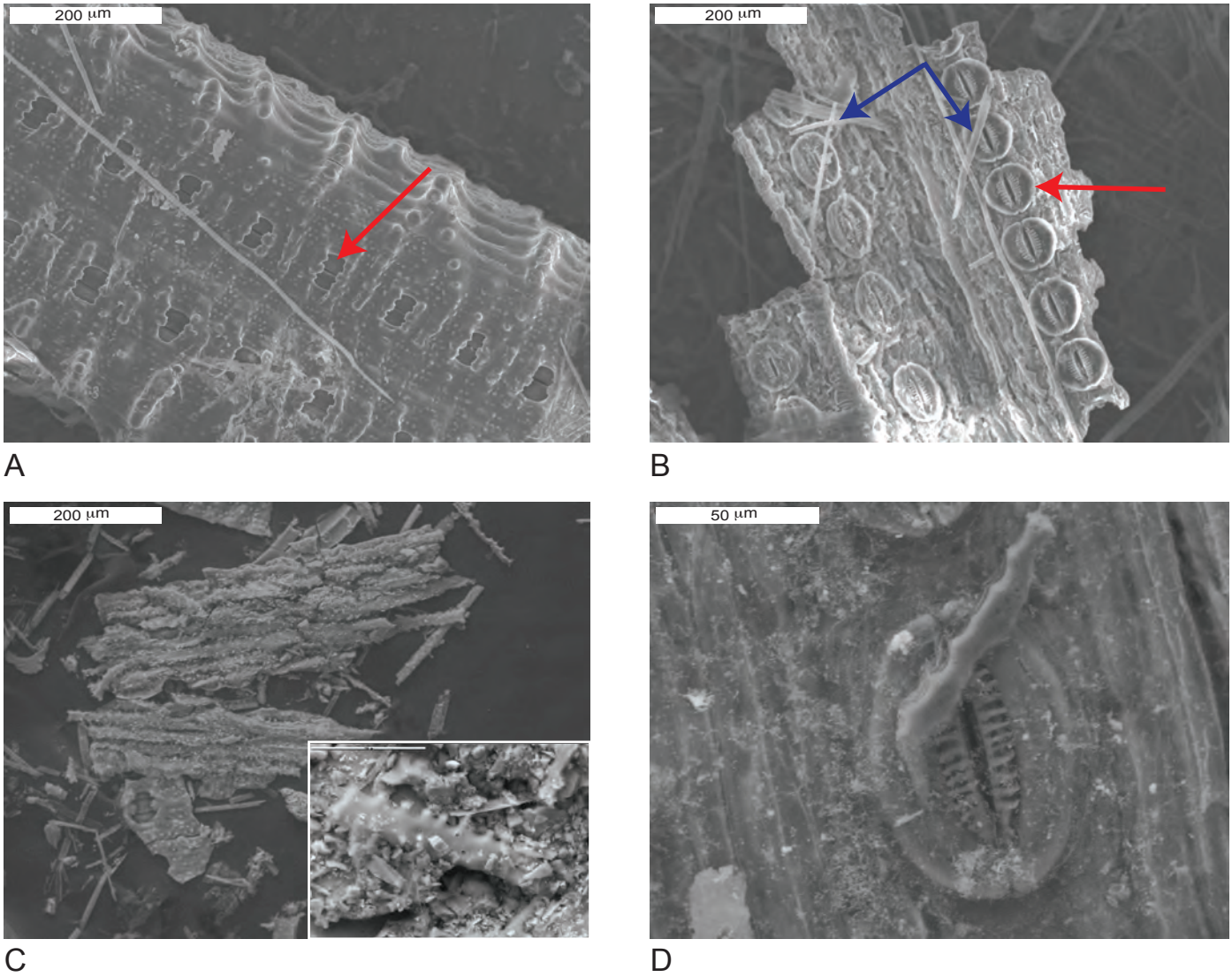

Figure 5—Horsetail (*Equisetum hyemale*) from the banks of the Rio Bonito, Lincoln County, NM, showing siliceous phytoliths. **A)** Outside of stem epidermal tissue showing stomatal openings (red arrow) amidst papillate and crenulated epidermis. The guard cells control the width of the stomatal slit. **B)** Inside of stem showing a line of siliceous stomata (red arrow). The stomatal guard cells have comb-like structures in their interiors. Acicular (needle) morphologies seen in several places (blue arrows). **C)** Crenulated edges of epidermal cells in parallel and acicular phytolith morphologies can be seen. In the background, cylindrical polylobate morphologies are almost too small to be noticed. Insert—High magnification of a single elongate echinate long-cell. **D)** High magnification of interior of a silicified stoma with the comb-like structure, which could be unique to this species. It is overlain by an individual cylindrical polylobate phytolith type.

the elemental chemistry and mineralogy of the phytoliths from these plants; 3) characterization of the morphological changes to biominerals during mechanical weathering and abrasion processes, and; 4) a comparison of all of these results to identified fragments of potential phytoliths and preserved plant-derived minerals from FSC sediments and Miocene-aged plant fossils from the RLF of the Barstow Formation.

Phytolith Morphology

Creosote and horsetail display completely different phytolith types from one another. Within each plant, there is a diversity of phytolith morphologies in both soft and woody tissues (Table 1). Creosote wood exhibits more morphologies than the leaves. The leaves have three main phytolith morphologies: globular echinate (Fig. 6A, 8A), cubic (Fig. 6A), and parallelepipedal (Fig. 6A). The woody tissue contains those same morphologies with the addition of tabular oblong (Fig. 4A, 4C, 6B, 7A, 9A-B) and pyramidal (Fig. 7A) phytoliths. Horsetail stem and leaf tissues were analyzed together and produced 6 different morphologies: elongate echinate long-cells (Fig. 5C, 7B), cylindrical polylobate (Fig. 5C-D, 6D), acicular (Fig. 5B-C, 6C, 7B), papillate and crenulated epidermal tissue (Fig. 5A, 5C, 7B), stomata (Fig. 5A-B, 5D, 6C, 7B, 8C), and comb-like structures (Fig. 5B, 5D, 6C, 8C) in the center of the stomata (Table 1).

Plants produce a diversity of biomineral morphologies as illustrated in Figure 1 from our larger plant data set not discussed in detail here (Table 1). Images 1A-D are from non-arid species, while 1E-F are from a riparian desert inhabitant. *Morus alba* leaves (mulberry, Fig. 1A) reveal a variety of morphological structures including silicified stomata and crenulated epidermis. Mulberry woody tissue (Fig. 1B) displays silicified vascular tissue with calcic cubic and parallelepipedal biominerals. EDX analysis (not shown in this study) reveals the presence of Si and Ca, in addition to K and Mg. *Ficus benjamina* (weeping fig) leaf tissue produces silicified favose epidermal tissue (Fig. 1C) in which calcic globular echinate minerals (Fig. 1D) can be seen in situ. Maximilian sunflower leaves (*Helianthus maximiliani*), a riparian plant from the southwestern USA, produce silicified hair cells and trichome bases (Fig. 1E), which are relatively large in size. Striations are observed on the surface of the hair cell (Fig. 1F).

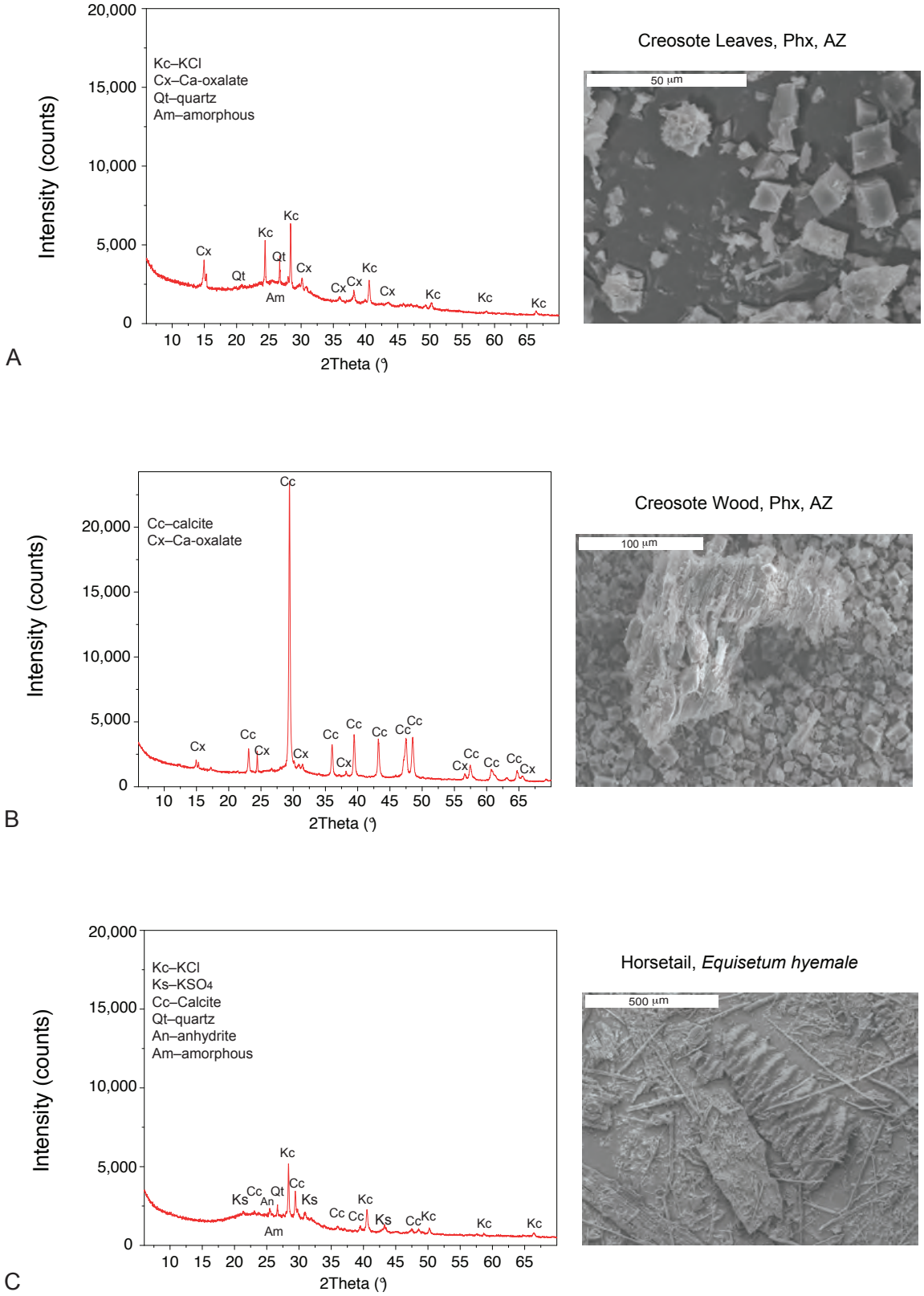

Figure 6—X-ray diffraction (XRD) pattern analysis of creosote and horsetail. **A)** Creosote Leaf mineralogy. There is a large amount of amorphous content, which produces the high background level above which peaks are visible. Individual mineral peaks include: potassium chloride (01-072-1540), 23%; calcium oxalate (whewellite, 01-078-6695), 62%; low quartz (01-087-2096), 15%. Large amounts of soluble salt minerals in the leaves may reflect the evapotranspiration-driven location of these materials, ion binding of calcium, osmotic control of the stoma opening, etc. SEM shows the characteristic rosettes (globular echinate), rhombohedra (parallelepipedal), and cubic crystallographies. **B)** Creosote Wood mineralogy: A large amount of calcite present in the wood as structural elements, in cubic, parallelepipedal, and tabular oblong phytolith morphologies. Note there is no amorphous material present. Minerals include: calcite (01-086-2334), 85%; calcium oxalate (whewellite, 01-078-6695), 15%; 1 small unidentified peak (at 17.2 on the X-axis). SEM shows monoclinic (tabular oblong) and cubic calcic phytoliths, some still in situ in a fragment of uncombusted wood, probably providing structure to the stomata. **C)** Horsetail Stem mineralogy. A large amount of amorphous material is present. Minerals include: potassium chloride (00-004-0587), 28%; calcite (01-086-2334), 24%; potassium sulfate (00-044-1414), 23%; calcium sulfate (anhydrite, 01-072-0503), 13%, and low quartz (01-087-2096), 12%. SEM shows the wide variety of morphologies in silica that are present in horsetail. Much of the horsetail stem is indurated with silica and thus remains after the ashing preparation.

Plant	Plant Part	Elements Present (EDX)	Crystalline Minerals Present (XRD)	Amorphous Material Present (XRD)
Creosote	Leaf	Si, Ca, C, O, K, Al, Mg, Cl	Whewellite (62%) Potassium Chloride (23%) Quartz (15%)	Yes (most likely Ca)
Creosote	Wood	Ca, C, O, K, P, Mg	Calcite (85%) Whewellite (15%)	No
Horsetail	Stem and leaf	Si, Ca, C, O, K, S, P, Al, Cl	Potassium Chloride (28%) Calcite (24%) Potassium sulfate (23%) Anhydrite (13%) Quartz (12%)	Yes (most likely Si)
Mulberry	Leaf and Wood	Si, Ca, C, O, K, Al, Mg, Cl	N/a	N/a
Weeping Fig	Leaf	Si, Ca, C, O, K, Mg, Na	N/a	N/a
Maxi-millian's sunflower	Leaf	Si, Ca, C, O, K, S, Al, Mg, Cl, Na	N/a	N/a

Table 2—Overview of elemental composition and mineralogy of plants in this study.

Chemistry and Mineralogy

Calcium biominerals are dominant in creosote, while amorphous silica is the primary mineral substance identified in the horsetail. In the creosote, calcic phytoliths dominate the woody tissue, while a mix of amorphous and crystalline phytoliths are in the leaves.

Creosote leaf XRD patterns reveal a large amount of amorphous material and smaller amount of crystalline minerals (Fig. 6A). Of the crystalline material, the majority of the crystals are whewellite (62% of crystal material), followed by potassium chloride (23%) and quartz (15%). EDX confirms Ca, C, O and K are present (Fig. 8A) Other EDX spectra, not shown, included the presence of Ca, C, O, K, Cl, Mg, Si, and Al. Creosote wood XRD patterns show the crystalline calcium minerals calcite and whewellite. Calcite is the predominant crystalline material at 85% of total crystals and the calcium oxalate mineral whewellite is 15% (Fig. 6B). EDX spectra not shown, confirmed the presence of Ca, C, O, K, P, and Mg. Horsetail whole stem XRD patterns reveal predominantly amorphous material, with smaller amounts of crystalline minerals present (Fig. 6C). Of the crystalline material, 28% of the crystals are potassium chloride, 24% calcite, 23% potassium sulfate, 13% anhydrite and 12% quartz. EDX spectra display Si, C, O, Ca, and K peaks (Fig. 8C). Other EDX analyses not shown here contained the presence of Ca, C, O, S, P, K, Cl, and Al. Table 2 displays the chemistry and mineralogy of all plants in this study.

In our larger plant phytolith reference library, *Morus alba* (mulberry) EDX analyses of the leaf and woody tissue reveal the presence of several elements including C, Si, O, Ca, K, Al, Mg, and Cl. *Ficus benjamina* (fig) EDX of leaf tissue indicate C, O, Ca, K, Si, Mg, and Na. *Helianthus maximiliani* (Maximilian's sunflower) contains Si, Ca, C, O, K, S, Na, Al, Cl and Mg demonstrated with EDX analysis.

Mechanical Weathering Simulation Experiments

The mechanical weathering simulation of the plant biomineral products at successive time steps from five seconds to five minutes yielded recognizable morphologies at all time steps (Fig. 7A). Cubic, parallelepipedal, tabular, oblong, pyramidal and globular echinate morphologies (Fig. 7A) from creosote sustained varying amounts of damage to their structures. A globular echinate morphology was still in good condition after one minute of simulated weathering (Fig. 4D), but only somewhat recognizable after two minutes, where the twinned crystals are separating out of their rosette, yet the individual crystals remain intact (Fig. 7A, 120 seconds). The cubic, parallelepipedal, tabular oblong, and pyramidal morphologies are identifiable at all time steps (Fig. 4A-C; Fig. 7A; Fig. 9A-B), with some pitting and cracking observed. Rounding of pointed surfaces was also frequently observed. This type of simulated mechanical weathering broke up the silicified plant remains of the horsetail. Nevertheless, individual cellular cavities, acicular bodies, globular echinate long-cells, guard cells, stomatal coverings and stomatal remains from horsetail were all identifiable at all time steps (Fig. 7B).

Sediment and Fossil Comparisons

The Fort Stanton Cave sediment (Fig. 2D) was analyzed in several stages. Separation of the sediments by particle size yielded 80% silt, 19% clay, and less than 1% sand indicating that the depositional environment was low energy. Initially, the first observations of the untreated and unseparated sediments yielded potential biominerals, one of which looked similar to a weathered globular echinate morphology and contained a Ca-Mg-C-O chemical signature (Fig. 8B), however no precise plant identification could be made from it. After separation, potential biominerals were found in the silt size fraction, a couple of which appear similar to guard cells in stomata and are composed of silica (Fig. 8D), but the plant family or genus could not yet be identified. The Barstow Formation rock samples that contained visible plant fossils (Fig. 2E) exhibited positive imprints of biomineral pyramidal and cubic morphologies in an organized pattern parallel to the fossil imprint (Fig. 9C-D) The EDX revealed the presence of Fe, O, Si, C, Cl, and Ca in the fossilized portion of the sample (Fig. 9F), while the bedrock geochemistry indicates a complex mixture of limestone, conglomerate, sandstone, siltstone and, shale (Fig. 9E).

Discussion

In this study, there was a diversity of phytolith morphologies present in both study plants (Table 1). The large variability of phytolith morphologies within creosote shows that it uses multiple plant parts to make different minerals and that noncrystalline material is important in leaf tissue. Globular echinate, cubic, and parallelepipedal morphologies were found in both leaf and woody tissue. Woody tissue also displayed tabular oblong (monoclinic) and pyramidal morphologies. Why is there such a large diversity in morphology in these plants? Biomolecules and bio-structures have been observed to affect Ca^{2+} oxalate crystal shapes inside the vacuoles (Bauer et al. 2011). Thus, gross morphology on the cellular level may be a significant part of the explanation. A large amount of both Si and Ca amorphous material in leaf tissue appears to be lining cells and stomata. Perhaps

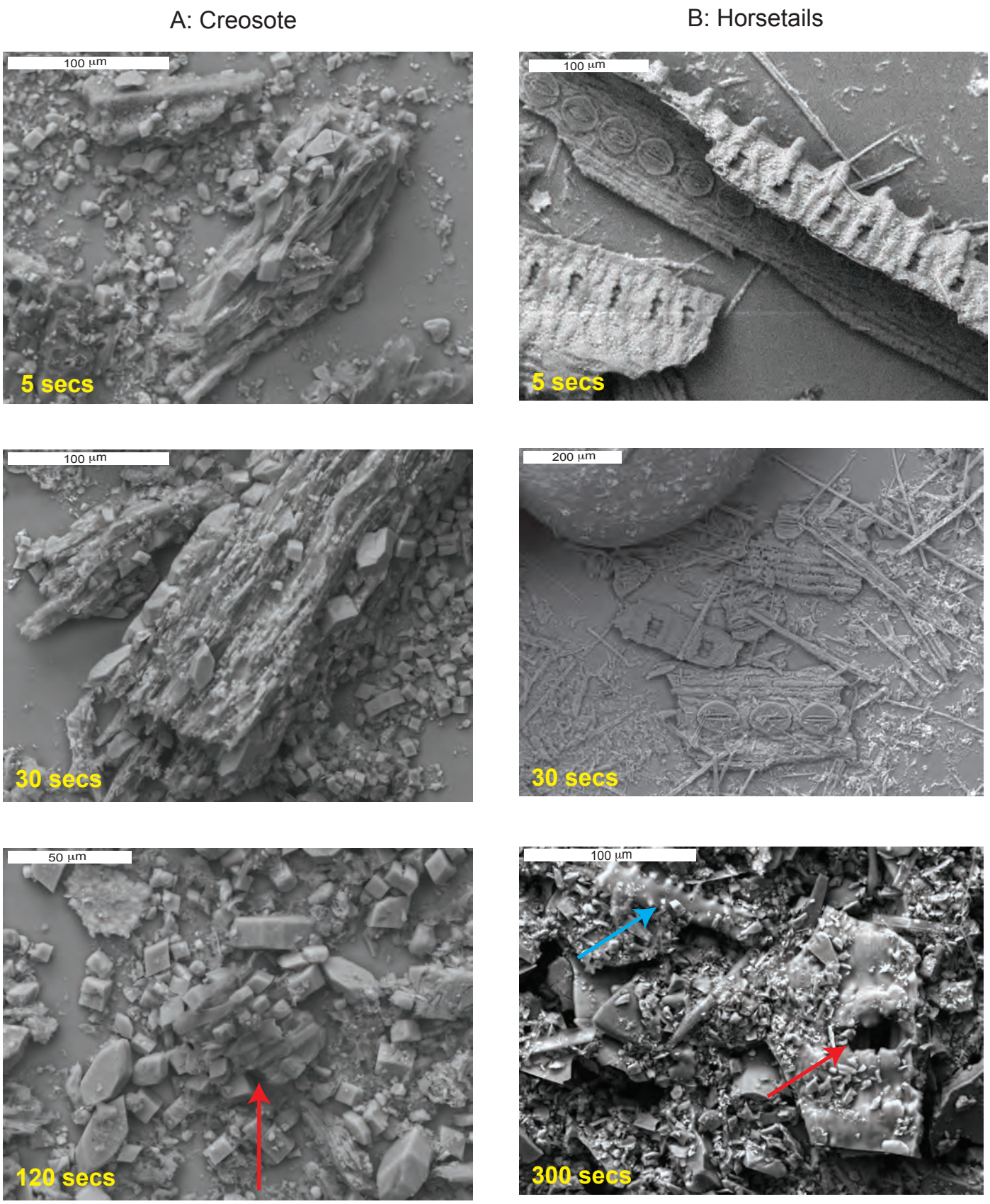

Figure 7—Simulated mechanical weathering experiments: **Panel A—Creosote** at 3 timesteps: *Timestep* 1 (5 secs) showing tabular oblong monoclinic crystals still in situ within epidermal tissue, showing signs of cracking; *Timestep* 2 (30 secs) tabular, rhombohedra and cubic crystals still in place within tissue, not much wear can be seen; *Timestep* 3 (120 secs) crystals liberated from tissue, some breakage, but many crystals still intact with some rounding and pitting on the crystal surfaces. Featured in the center is a twinned rosette (globular echinate) showing individual crystals (red arrow points to bottom of rosette). **Panel B—Horsetail** at 3 timesteps: *Timestep* 1 (5 secs) intact crenulated and papilliate epidermis on stem outer surface and row of stomata lining interior of stem; *Timestep* 2 (30 secs) acicular (needle) cells beginning to separate from epidermis, stomata still intact. Ottawa sand grain (grinding medium) visible in upper left; *Timestep* 3 (300 secs) stomatal structures beginning to separate from epidermis and break apart, stomatal slit still recognizable (red arrow). Within the debris, an elongate echinate long-cell is recognizable (blue arrow), but showing signs of weathering.

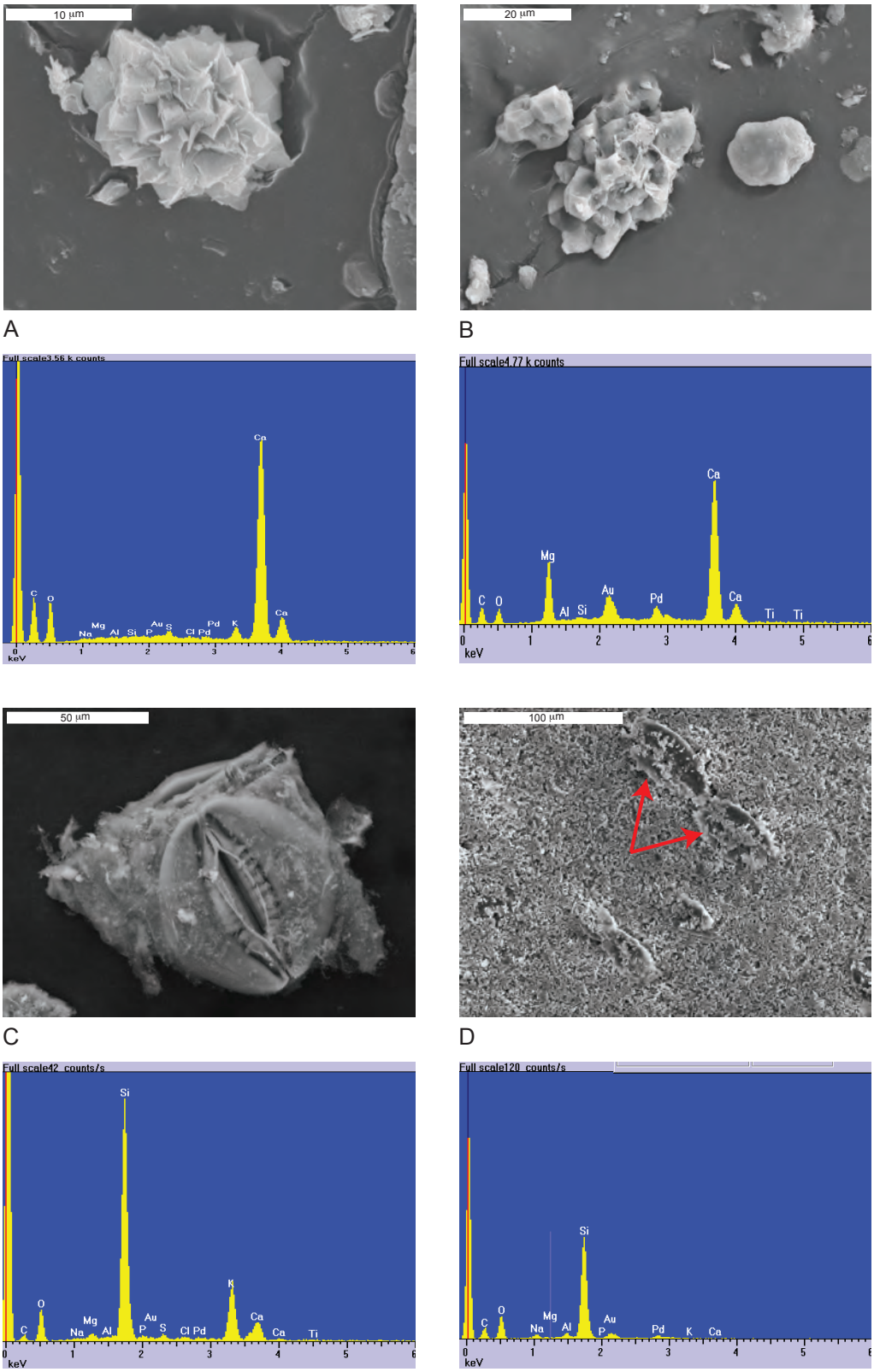

Figure 8—Comparison of modern phytoliths to potential biominerals from cave mud deposits from Fort Stanton Cave. A) Creosote leaf tissue contains globular echinate (rosette) phytolith morphology with a calcium mineral chemistry indicated by the energy dispersive x-ray spectrum (EDX). B) Mud Deposits from unprocessed sediment sample from Snowy River South within Fort Stanton Cave, Lincoln County, NM. Object resembling a highly weathered phytolith, probably a globular echinate morphology, of calcic composition, with Mg also present. C) Stoma from ashed modern horsetail and EDX spectrum indicates silica dominant structures, with Ca, C, K and Mg also present. D) Mud deposits from the Mud Mushroom formations in Fort Stanton Cave, Lincoln County, NM. Features resembling stoma (red arrows) covered in silt, in a sample that was treated with sodium hexametaphosphate. EDX spectrum indicates it is a silica structure with a small amount of carbon.

the extraordinary longevity of living creosote clones and the availability of calcium and other minerals in arid environments has allowed this plant to compartmentalize only calcic minerals into its woody tissue, which persists over many decades and perhaps centuries or beyond (Vasek 1980). Less crystalline mineral or amorphous substances likely line its leaf tissues, which are regularly replaced. The tabular oblong (monoclinic) phytoliths in the woody tissue appear to provide structure to the stomatal openings (Fig. 6B).

Interestingly, a number of plant-derived minerals were identified in the two species of climatically relevant modern plants, creosote and horsetail. Both amorphous and crystalline quartz, as well as potassium chloride, were present within samples from both plants. Moreover, although creosote woody tissue yields only crystalline materials, leaf tissues of both study plants contain both amorphous and crystalline material. Biominerals are precipitated in both amorphous and crystalline mineral forms; however, in some species, the amorphous material matures over time into crystalline minerals, the degree of which depends on the stability of the amorphous material (Addadi et al. 2003; Bauer et al. 2011). Calcic minerals are found in both plants studied, but each plant had different calcic mineral signatures. Creosote possesses whewellite, which is absent in the horsetail, however both plants produce calcite. Calcium and potassium sulfate minerals are both produced by the horsetail, but absent in the creosote. EDX analyses reveal the presence of Mg, P, Al, and Na in plant samples, indicating that these elements also have a role in plant functions and accumulate in phytoliths. Interestingly, in most literature, we have not found mention of specific calcic phytoliths in horsetails, although other elements were reported as present (Neumann et al. 2010). Great emphasis is placed on the variety of silica bodies produced by horsetail (Florea et al. 2008; Law and Exley 2011; Yamanaka et al. 2012) including incorporation of other metals into tissues and presumptively into minerals.

Horsetail primarily utilizes amorphous silica within its internal and epidermal structures; however, this is supported by a variety of other crystalline minerals such as quartz, potassium chloride, potassium and calcium sulfates, and calcite (Fig. 5 A-D; Fig. 6C). What roles these other minerals play remains unclear. Their presence may simply reflect the need to have a repository for materials that the plant takes up in the normal course of imbibing water from the roots (Brooks et al. 1981; Bauer et al. 2011; Law and Exley 2011; Yamanaka et al. 2012) or they may serve some specific purpose in the physiology of the plant (Bauer et al. 2011; Law and Exley 2011; Yamanaka et al. 2012). In addition to papillate and crenulated epidermal tissue and a multitude of cells and stomata lined with silica, horsetails produce elongate echinate long-cells, cylindrical polylobate, and acicular phytolith morphologies (see Fig 5A-D for examples of these shapes).

Both plants studied in this report have epidermal and stomatal tissue remaining after ashing, but are distinct from each other in size, morphology, and chemistry. The large amount of calcareous minerals present in creosote seems to support the idea that desert plants may also play a large role in the storage and release of calcium in arid environments, as has been suggested for plants in other ecosystem types (Monje and Baran 2004; Street-Perrott and Barker 2008; Borrelli et al. 2009). Brown et al. (2013) found that in 12 species of Acacia, calcium oxalate crystal morphologies were not affected by rainfall amounts, but distribution and the amount of crystals were affected by climate and available Ca in the soil. It is possible that creosote could be similarly affected.

Both study plants revealed biominerals that are distinct from one another and should be compared to other known phytoliths to determine if they can be used as genus or species identifiers and environmental indicators. For example, a related horsetail species, *Equisetum arvense*, is known for its silica-indurated tissues, but has stomata that are distinct and visually different from *Equisetum hyemale* used in this study (Law and Exley 2011). There is no known literature about creosote phytoliths, but all of the morphological shapes observed within the plant are listed as phytolith types in the systematics literature (Madella 2005; Piperno 2006), and factors such as size and chemistry may hold the key to individual species' phytolith biosignatures.

In much of the existing phytolith literature, the term "phytolith" has been primarily or exclusively applied to biominerals of a silica composition (Piperno 2006). This may be because many of the extraction methodologies in use are highly destructive to calcic and other biominerals, thus they were not appearing in such datasets. However, non-silica biominerals are widely distributed and important in plants, therefore consideration of phytoliths as exclusively silica-based biominerals limits the amount of information that can be determined. Silica bodies are detected more easily when optical microscopy is the only visualization method available, which may explain the emphasis on that composition. Optical microscopy is useful in terms of time, source materials, cost considerations, etc. in studies and provides insightful information about phytoliths, while scanning electron microscopy provides a more detailed look at phytolith surface features, dimensions, and includes elemental composition capability, and both methods need more data to better understand phytolith potential. Methods of preparation designed to isolate silica phytoliths are meant to chemically remove minerals such as calcium-containing compounds and organics, which would also destroy plant-derived minerals of those compositions. Care needs to be taken when liberating phytoliths from modern plant materials and when isolating and interpreting them from sediments and geologic samples. Too much heat from dry ashing, wildfires, or ancient human preparation (cooking, baking, etc.) could potentially dehydrate the phytoliths resulting in chemical changes (Fig. 3).

Mechanical Weathering

Both study plants yielded identifiable phytolith morphologies after the simulated mechanical weathering treatments, suggesting that significant preservation of phytoliths is possible after such processes. Cubic, parallelepipedal, tabular oblong, and pyramidal morphologies (calcic minerals) from the creosote remained the most recognizable after the simulated weathering treatments. The silicified epidermal and stomatal tissue of the horsetail was also identifiable after all grinding steps. The more delicate features of phytoliths with globular echinate, acicular, cylindrical polylobate and globular echinate long-cell morphologies were damaged during weathering simulation, but the resulting fragments remained identifiable, suggesting that well weathered phytoliths may still be identifiable in field sites that are unprotected from weathering processes. Cracking, pitting, separation of cellular tissue, rounding, and breakage of pointed appendages were visible after experimental weathering. The Ottawa sand grains themselves were only somewhat damaged after this treatment. The size difference between the sand (about 2 mm diameter) and the phytoliths (10–200 microns) seem to positively affect their ability to survive weathering because the chances of any individual phytolith being crushed by a sand grain is balanced by the likelihood of a phytolith falling into the spacious voids between the large grains. Results of simulations using smaller grained sediments might differ in this regard, and perhaps be more destructive to phytoliths. This should be tested further.

Factors affecting phytolith survivability include their morphology, composition, and the physical and chemical characteristics of the depositional environment (Piperno 2006; Cabanes et al. 2011). For example, survival of delicate structures during sediment transport depends on particle size and shape, the amount of clay and silt present in the bedload, and perhaps other unknown factors (Granados-Sánchez et al. 2011), which seemed to be evident from our study results as well.

In the arena of chemical weathering, the presence of Al and Fe oxides can affect the degree of survivability of phytoliths because they can reduce the amount of dissolved silica available in soils. There is generally more free dissolved Si in acidic environments or when there is more water available in the

Larrea tridentata (creosote)

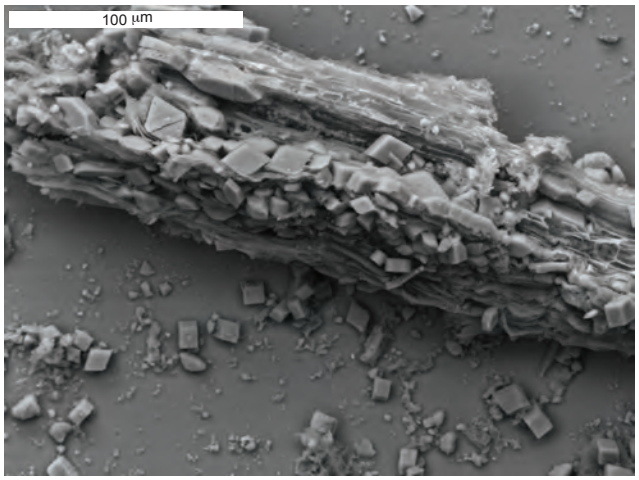

A

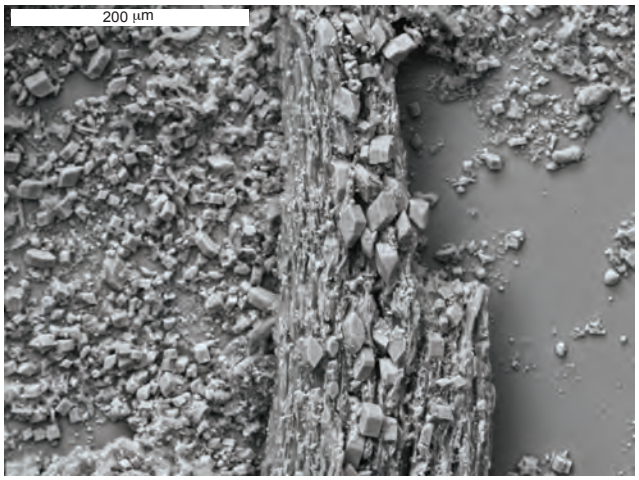

B

Barstow fossil plant remains

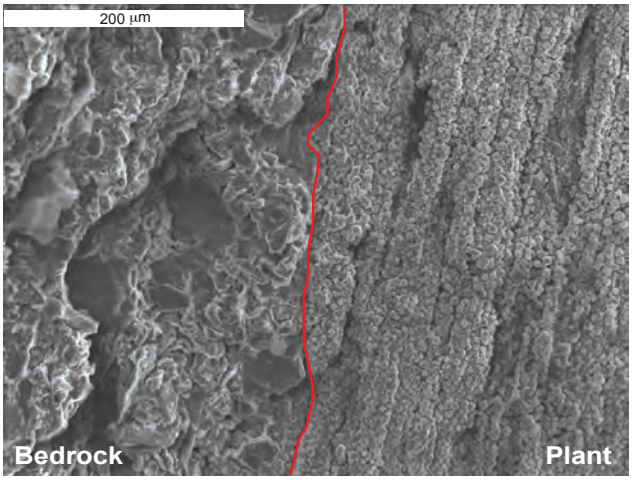

C

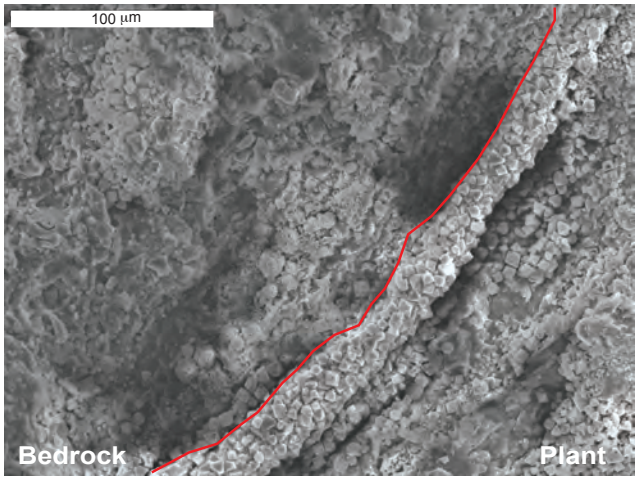

D

Barstow fossil elemental composition

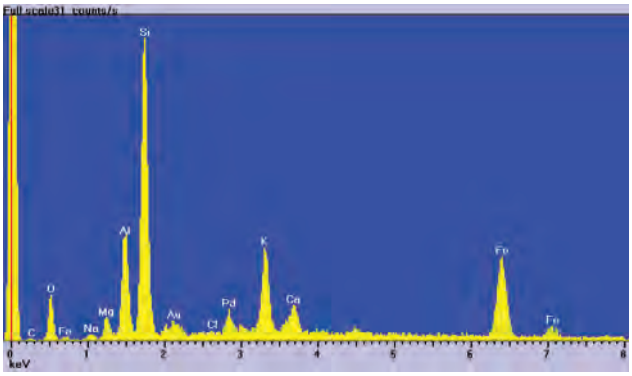

E

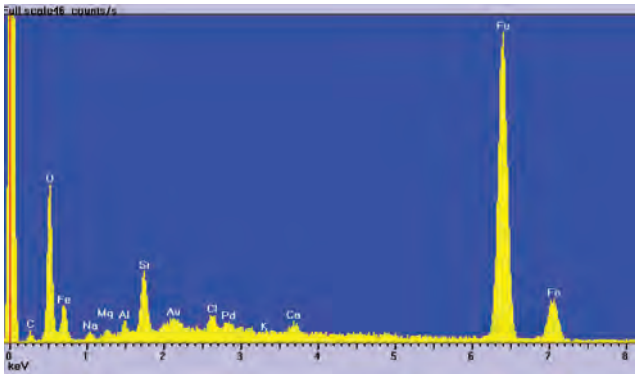

F

Figure 9—The common cubic, parallelepipedal, and tabular oblong morphologies of calcic phytoliths in arid environments can be seen in the following comparison of Miocene-aged plant fossils from the Barstow Formation, California, with modern creosote wood. **A)** Modern creosote wood showing cubic, parallelepipedal, and tabular oblong calcic phytoliths in situ, some have cracked from simulated mechanical weathering. **B)** Tabular oblong phytoliths lined up within the cellular matrix of modern creosote wood. **C)** Miocene-aged fossil plant from the Rainbow Loop Flora (see also Fig. 2 E). Small cubic and pyramidal phytolith shapes encrust the longitudinal fossilized plant fibers in the right half of the image, while the contrasting rock texture can be viewed on the left, the boundary marked by the red line. D) Miocene-aged fossil plant from the same formation. Higher magnification of the rock and plant boundary is indicated by the red line. The bedrock is from a deltaic deposit into lacustrine (lake) sediments. E) The EDX spectrum of the bedrock (to the left in C and **D)** indicates a complex mixture of limestone, conglomerate, sandstone, siltstone and shale. F) The EDX spectrum of the plant fossil reveals a significant amount of Fe, which probably was a secondary mineralization of the decomposing plant tissue with calcic and silicic phytoliths that are now coated by iron oxides.

soil, yet the presence of Al and Fe may negate this completely due to the formation of Al and Fe oxides and clays within the soil (Piperno 2006). If that occurs, then the amount of dissolved Si in an acidic environment would be less, and thus the dissolution of Si phytoliths would be greater. The extent to which biogenic silica reacts with Al and Fe oxides remains unclear (Street-Perrott and Barker 2008). Calcium based or other non-silica biominerals within sediments and other depositional environments have not been studied for survivability potential.

Preservation and Climate Indications

Phytoliths are useful geobiological microstructures that can be preserved through time as indicators of surface vegetation, climate, moisture regimes, and as contributors to the global cycling of silica and carbon. Microbial interactions during plant decay can transform plant-derived minerals; for example, in saguaros, weddellite is converted to calcite with the help of microbes. The decay of saguaro cactus added 2.4 grams of inorganic carbon per square meter per year to desert soil (Garvie 2003), which effectively sequesters atmospheric carbon, another potential role of calcic phytoliths. Certainly, the horsetail must play a role in silica cycling (Conley 2002; Street-Perrott and Barker 2008; Law and Exley 2009) because this plant group is widely distributed globally and is of long antiquity; however, the precise role of horsetails in silica cycling has not yet been studied.

Episodic flooding and sediment deposition into karst systems like Fort Stanton Cave, could deposit phytoliths into an environment protected from surface weather, UV radiation, and humidity changes. Both siliceous and calcic bodies were present in the FSC sediments, indicating preservation potential of both mineral compositions. Reinhard and Danielson (2005) found Agavaceae and Cactaceae phytoliths in coprolites and on dental samples from southwest archaeological sites both on the surface and in caves, supporting good preservation of these minerals. In our study, completely unprocessed sediment and fossil samples observed under SEM yielded identifiable general morphologies in both modern and fossilized material, yet could not be linked to a specific plant genus or species. The existing North American phytolith database is very incomplete, so it is possible that positive identification can happen at a later time. We attempted to document many plant species in our larger phytolith database (not shown here), in order to have a reference library for comparison to fossil materials, but much work remains.

Abundant Fe-oxides present in the plant fossils of the Miocene Barstow formation indicate that the original plant material was replaced, in part at least, by Fe-oxides. However, calcic signatures are still detectable in the EDX, and crystalline morphologies remain as Fe-oxide pseudomorphs of the phytolith crystals. This suggests that long term preservation of calcic phytoliths is possible and that these biominerals may be just as important as silicate bodies in paleobotanical studies and should not be overlooked.

Identification of genus or species-specific, unique phytoliths can be used as localized ecological biosignatures where such data exists. For example, horsetails are indicators of riparian environments, localized water sources within arid climates, or on the other hand, of a generally wet climate. Fossil Equisetales from Patagonia have been found of Jurassic age (Channing et al. 2011) suggesting that this group has a very long history. Contrastingly, creosote, originally indigenous to South America, is a well-known warm climate, arid-adapted plant, dominant in all three hot North American deserts, and known for longevity of individual specimens (Vasek 1980). Both plants produce biominerals that could be useful in determining age of their establishment and development within North America, as well as serve as an indication of local environmental conditions.

New Mexico has 65 million years of plant development and evolution that has produced the flora that we see today, flora that has been influenced by geological events, climate, moisture availability, and source material and terrain. Ecological evolutionary indicators are not necessarily well represented, and interpretations of the available data can prove difficult. The North American Deserts are thought by some to be relatively recent, about 10,000 years old (Baldwin 2002), although earlier deserts developed in previous interglacials (Van Devender et al. 1984). The first indications of drying of the area dates back to 5 million years ago. The lack of fossilized arid land plants such as creosote, Cactaceae, and Fouquieriaceae makes it difficult to determine their age and establishment in North America, old or modern (Baldwin 2002). Holocene studies of *Neotoma* (packrat) middens (Van Devender et al. 1984; Betancourt et al. 2001) suggest a piñon-juniper woodland dominated south-central New Mexico and a lack of Chihuahuan Desert plants, while Wells (1979) presents midden evidence showing the coexistence of woodland conifers and evergreen oaks, with aridland plants including *Nolina*, *Lechuguilla*, *Dasyliron*, *Opuntia macrocenta*, and *Berberis trifoliata* in the now current range of the Chihuahuan Desert. Microfossil phytoliths can potentially shed light on some of the conflicting midden studies and help to yield a clearer picture of the climate and ecology of the region. The presence (or absence) of either creosote or horsetail phytoliths within the middens could confirm the likely moisture regime of the time.

Conclusions

Modern plants in this study revealed multiple distinguishable phytolith morphologies and compositions that were still identifiable after simulated mechanical weathering experiments. As expected, silica was the dominant biomineral in the horsetail, while calcareous minerals were dominant in the creosote. Additionally, several other minerals were present within the study plants, indicating other important elements for plant functions. Several potential fossilized mineral bodies were identified in both Fort Stanton Cave sediments and in the Miocene-aged Barstow Formation fossils, suggesting long-term preservation of phytoliths, although exact plant genus or species could not be linked with the phytoliths. These microfossils could be added to the suite of biological signatures for use in interpreting previous climate conditions reflected in the composition of surface vegetation. Additionally, phytolith analysis could be of use in understanding the chronology of invasion of various plant species into an area. North American phytolith data is limited and more plant species should be investigated for better understanding and comparison to fossilized samples.

Acknowledgments

The authors thank the National Cave and Karst Research Institute and Dr. Van Romero (NM Tech) for research support. Thanks also go to the NMT Graduate Student Association for travel funds for the first author. In addition, the authors are grateful to Mr. Stas Edel for photography and field assistance, Mr. Wayne Walker and the Fort Stanton Cave Study Project for help with cave sampling, to Dr. Virgil Lueth for access to the XRD instrument, to Mr. Fred Hanson for assistance with sample preparation, to Mr. Jason Walz of the USDA Forest Service - Lincoln National Forest for access to plant samples, and to the Bureau of Land Management for access to Fort Stanton Cave and to Dr. Kenneth Ingham for Fort Stanton Cave photography. Finally, the authors are very thankful to the senior author's committee members, Dr. Becky Bixby, Dr. Peter Mozley, and Dr. Bruce Harrison for all of their guidance and suggestions.

References

Addadi, L. Raz, S. and Weiner, S., 2003, Taking advantage of disorder: Amorphous calcium carbonate and its roles in biomineralization, Advanced Materials, v. 15(12), pp. 959-970.

Andrews, M.Y., Ague, J.J., and Berner, R.A., 2008, Weathering of soil minerals by angiosperm and gymnosperm trees, Mineralogical Magazine, v. 72(1), pp. 11-14.

Baldwin, B.G., editor, 2002, The Jepson desert manual: Vascular plants of southeastern California, University of California Press, 624 pp.

Bauer, P., Elbaum, R., and Weiss, I. M., 2011, Calcium and silicon mineralization in land plants: Transport, structure and function, Plant Science, v. 180, pp. 746-756.

Betancourt, J.L., Rylander, K.A., Peñalba, C., and McVickar, J.L., 2001, Late Quaternary vegetation history of Rough Canyon, south-central New Mexico, USA, Palaeogeography, Palaeoclimatology, Palaeoecology, v. 165, pp. 71–95.

Borrelli, N., Honainea, M.F., Altamiranoa, S.M. and Osterrieth, M., 2011, Calcium and silica biomineralizations in leaves of eleven aquatic species of the Pampean Plain, Argentina, Aquatic Biology, v. 94, pp. 29-36.

Bowers, J. E., 1993, Shrubs and trees of the southwest deserts, Western National Parks Association, Tucson, AZ, 140 pp.

Brook, G. A., Burney, D. A., and Cowart, J. B., 1990, Desert paleoenvironmental data from cave speleothems with examples from Chihuahuan, Somali-Chabli and Kalahari Deserts, Paleogeography, Paleoclimatology, Paleoecology, v. 76, pp. 311–329.

Brooks, R.R., Holzbecher, J. and Ryan, D.E., 1981, Horsetails as indirect indicators of gold mineralization, Journal of Geochemical Exploration, v. 16(1), pp. 21-26.

Brown, S. L., Warwick, N. W. M., and Prychid, C. J., 2013, Does aridity influence the morphology, distribution and accumulation of calcium oxalate crystals in Acacia (Leguminosae: Mimosoideae)? Plant Physiology and Biochemistry, v. 73, pp. 219–228.

Budel, B., Wessels, D.C.J., and Mollenhauer, D., 1993, Mass development of Nostoc microscopicum (Carmichael) Harvey ex Barnet & Flahault in a Cave in Clarens Sandstone of the Drakensberg Mountains, South Africa (Golden Gate Highlands National Park), Archives Protistenkd, v. 143, pp. 229–235.

Cabanes, D., Burjachs, F., Expósito, I., Rodríguez, Allué, E., Euba, I., and Vergès, J.M., 2009, Formation processes through archaeobotanical remains: The case of the Bronze Age levels in El Mirador Cave, Sierra de Atapuerca, Spain, Quaternary International, v. 193, pp. 160–173.

Cabanes, D., Mallol, C., Expósito, I., and Baena, J., 2010, Phytolith evidence for hearths and beds in the late Mousterian occupations of Esquilleu Cave (Cantabria, Spain), Journal of Archaeological Science, v. 37, pp. 2947–2957.

Cabanes, D., Weiner, S., and Shahack-Gross, R., 2011, Stability of phytoliths in the archaeological record: A dissolution study of modern and fossil phytoliths, Journal of Archaeological Science, v. 38, pp. 2480–2490.

Carrión, J. S., Munuera, M., Navarro, C., Burjachs, F., Dupré, M. and Walker, M.J., 1999, The palaeoecological potential of pollen records in caves: The case of Mediterranean Spain, Quaternary Science Reviews, v. 18, pp. 1061–1073.

Chauhan, D.K., Tripathi, D.K., Sinha, P., and Tiwari, S.P., 2009, Biogenic silica in some Pteridophytes, Bionaturae, v. 29, pp. 1–9.

Channing, A., Zamuner, A., Edwards, D. and Guido, D., 2011, Equisetum thermale Sp.. nov. (Equisetales) from the Jurassic San Agustin hot spring deposit, Patagonia: Anatomy, Paleoecology, and Inferred Paleoecophysiology, American Journal of Botany, v. 98(4), pp. 680–697.

Conley, D., 2002, Terrestrial ecosystems and the global biogeochemical silica cycle, Global Biogeochemical Cycles, v. 16(4), pp. 1121-1129.

Day, P. R., 1965, Particle fractionation and particle-size analysis, *in* Black, C.A., Evans, D.D., White, J.L., Ensminger, L.E., and Clark, F.E., eds. Methods of Soil Analysis, Part 1, no. 9, pp. 545-567.

Dibblee, T.W., Jr., 1967, Areal geology of the western Mojave Desert, California. Geological Survey Professional Paper no. 522, United States Government Printing Office, Washington D.C., 153 pp.

Dick-Peddie, W.A., 1993, New Mexico vegetation: Past, present, and future, Albuquerque: University of New Mexico Press, 244 pp.

Dodson, C., 2012, A guide to plants of the northern Chihuahuan Desert, University of New Mexico Press, Albuquerque, NM, 194 pp.

Driessens, F.C.M. and Verbeeck, R.K., 1990, Biominerals, CRC Press, Boca Raton, FL, 440 pp.

Florea, R.M., Stoica, A.I., Ionica, M., and Baiulescu, G.E., 2008, Differential accumulation of gold and other metals by plants, Revista de Chimie, v.59(9), pp. 1019-1021.

Fort Stanton Cave Study Project (FSCSP), S. Peerman, editor, 2014, Report on the activities of the April 26 – May 4, 2014 expedition of the Fort Stanton Cave Study Project, Revision 3.3, June 11, 2014. Accessed at http://www.fscsp.org/Private/docs/reports/index.html

Franceschi, V.R. and Nakata, P.A., 2005, Calcium oxalate in plants: Formation and function, Annual Review of Plant Biology, v. 56, pp. 41-71.

Frost, R.L. and Weier, M.L., 2003, Thermal treatment of weddellite—A Raman and infrared emission spectroscopic study, Thermochimica Acta, v. 406, pp. 221–232.

Frost, R.L. and Weier, M.L., 2004, Thermal treatment of whewellite—A Thermal analysis and Raman spectroscopic study, Thermochimica Acta, v. 409, pp. 75–87.

Gal, A., Brumfeld, V., Weiner, S., Addadi, L., and Oron, D., 2012, Certain biominerals in leaves function as light scatterers, Advanced Optical Materials v. 24, pp. OP77–OP83.

Gardea-Torresdey, J.L., Arteaga, S., Tiemann, K.J., Chianelli, R., Pingitore, N., and MacKay, W., 2001, Absorption of copper (II) by creosote bush (Larrea tridentata): Use of atomic and x-ray absorption spectroscopy, Environmental Toxicology and Chemistry, v. 20(11), pp. 2572-2579.

Gardea-Torresdey, J.L., Tiemann, K.J., Hernandez, A., Bibb, J., and Rodriguez, O., 1997, Adsorption of toxic metal ions from solution by inactivated cells of Larrea tridentata (creosotebush), Journal Hazard Substance Res v. 3, pp. 1–16.

Garvie, L. A. J., 2003, Decay-induced biomineralization of the saguaro cactus (Carnegiea gigantea), American Mineralogist, v. 88, pp. 1879-1888.

Gobetz, K.E. and Bozarth, S.R., 2001, Implications for late Pleistocene mastodon diet from opal phytoliths in tooth calculus, Quaternary Research, v. 55, pp. 115-122.

Granados-Sánchez, D., Sánchez-González, A., Granados Victorino, R.L., and Borja de la Rosa, A., 2011, Ecología de la vegetación del Desierto Chihuahuense, Revista Chapingo Serie Ciencias Forestales y del Ambiente, v. XVII, pp. 111-130.

Katz, O., Cabanes, D., Weiner, S., Maeir, A.M., Boaretto, E., and Shahack-Gross, R., 2010, Rapid phytolith extraction for analysis of phytolith concentrations and assemblages during an excavation: An application at Tell es-Safi/Gath, Israel, Journal of Archaeological Science, v. 37, pp. 1557-1563.

Koch, K., Bhushan, B., and Barthlott, W., 2009, Multifunctional surface structures of plants: An inspiration for biomimetics, Progress in Materials Science, v. 54, pp. 137-178.

Kurmann, M.H., 1985, An opal phytolith and palynomorph study of extant and fossil soils in Kansas (U.S.A.), Paleogeography, Paleoclimatology, Paleoecology, v. 49, pp. 217-235.

Land, L., 2012, Geophysical prospecting for new cave passages: Fort Stanton Cave, New Mexico, USA, Carbonates Evaporites, v. 27, pp. 97-102.

Law, C., and Exley, C., 2011, New insight into silica deposition in horsetail (Equisetum arvense), BMC Plant Biology, v. 11, pp. 112-120.

Madella, M., Alexandre, A., and Ball, T., 2005, International code for phytolith nomenclature 1.0, Annals of Botany, v. 96, pp. 253-260.

Martin, W.C. and Hutchins, C.R., 1980, A flora of New Mexico. 2 Volumes, 2591 pp.

Mazumdar, J., 2011, Phytoliths of Pteridophytes, South African Journal of Botany, v. 77, pp. 10-19.

Monje, P.V. and Baran, E.J., 2004, Complex biomineralization pattern in Cactaceae, Journal of Plant Physiology, v. 161, pp. 121-123.

Mulholland, S. C. and Rapp, Jr., G., 1992, Phytolith systematics: An introduction. In Phytolith Systematics: Emerging Issues, Plenum Press, New York and London, pp. 1-14.

Neumann, M., Wagner, S., Noeske, R., Tiersch, B., and Strauch, P., 2010, Morphology and structure of biomorphous silica Isolated from Equisetum hyemale and Equisetum telmateia, Verlag der Zeitschrift furNaturforschung, v. 65b, pp. 1113-1120.

Parr, J.F., 2002, A comparison of heavy liquid floatation and microwave digestion techniques for the extraction of fossil phytoliths from sediments, Review of Palaeobotany and Palynology, v. 120, pp. 315-336.

Parr, J.F., Dolic, V., Lancaster, G. and Boyd, W.E., 2001, A microwave digestion method for the extraction of phytoliths from herbarium specimens, Review of Palaeobotany and Palynology, v. 116, pp. 203-212.

Perry, R.S., McLoughlin, N., Lynne, B.Y., Sephton, M.A., Oliver, J.D., Perry, C.C., Campbell, K., Engel, M.H., Farmer, J.D., Brasier, M.D., and Staley, J.T., 2007, Defining biominerals and organominerals: Direct and indirect indicators of life, Sedimentary Geology, v. 201, pp. 157-179.

Pinales, L.A., Chianelli, R.R., Durrer, W.G., Pal, R., Narayan, M., and Manciua, F. S., 2010, Spectroscopic study of inhibition of calcium oxalate calculi growth by Larrea tridentata, Journal of Raman Spectroscopy, v. 42, pp. 259-264.

Piperno, D. R., 2006, Phytoliths: A comprehensive guide for archaeologists and paleoecologists, Alta Mira Press, Oxford, UK, 238 pp.
Prychid, C.J. and Rudall, P.J., 1999, Calcium oxalate crystals in monocotyledons: A review of their structure and systematics, Annals of Botany, v. 84, pp. 725-739.
Raven, J.A. and Giordano, M., 2009, Biomineralization by photosynthetic organisms: Evidence of coevolution of the organisms and their environment. Geobiology, v. 7, pp. 140-154.
Reinhard, K.J. and Danielson, D.R., 2005, Pervasiveness of phytoliths in prehistoric southwestern diet and implications for regional and temporal trends for dental microwear, Journal of Archaeological Science, v. 32, pp. 981–988.
Reynolds, R.E., and Schweich, T.A., 2013, The Rainbow Loop Flora from the Mud Hills, Mojave Desert, California, Desert Symposium Field Guide and Proceedings, April 2013, pp. 39–48.
Romero, O. E., Lange, C. B., Swap, R., and Wefer, G., 1999, Eolian-transported freshwater diatoms and phytoliths across the equatorial Atlantic record: Temporal changes in Saharan dust transport patterns, Journal of Geophysical Research, v. 104(2), pp. 3211–3222.
Skinner, H.C.W., 2005, Biominerals, Mineralogical Magazine, v. 69(5), pp. 621–641.
Smith, A.R., Pryer, K.M., Schuettpelz, E., Korall, P., Schneider, H., and Wolf, P.G., 2006, A classification for extant ferns, Taxon, v. 55, pp. 705–731.
St. Clair, L.L., and Rushforth, S.R., 1976, The diatoms of Timpanogos Cave National Monument, Utah, American Journal of Botany, v. 63(1), pp. 49-59.
Street-Perrott, F. A., and Barker, P.A., 2008, Biogenic silica: A neglected component of the coupled global continental biogeochemical cycles of carbon and silicon, Earth Surface Processes and Landforms, v. 33, pp. 1436-1457.
Twiss, P.C., Suess, E., and Smith, R. M., 1969, Morphological classification of grass phytoliths, Soil Science Society of America Proceedings, v. 33(1), pp. 110-114.
Twiss, P.C., 1992, Predicted world distribution of C3 and C4 grass phytoliths, in Phytolith Systematics: Emerging Issues, Plenum Press, New York and London, pp. 113–128.
Van Devender, T.R., Betancourt, J.L. and Wimberly, M., 1984, Biogeographic implications of a packrat midden sequence from the Sacramento Mountains, south-central New Mexico, Quaternary Research, v. 22, pp. 344–360.
Vasek, F. C., 1980, Creosote-bush: Long-lived clones in the Mojave Desert, American Journal of Botany, v. 67(2), pp. 246–255.
Weisner, R.H. and the Upper Hondo Watershed Coalition, 2004, Upper Hondo Watershed Restoration Action Strategy, 2nd Edition. From the New Mexico Environmental Department web-site: www.nmenv.state.nm.us
Wells, P.V., 1979, An equable glaciopluvial in the west: Pleniglacial evidence of increased precipitation on a gradient from the Great Basin to the Sonoran and Chihuahuan Deserts, Quaternary Research, v. 12(3), pp. 311-325.
Yamanaka, S., Sato, K., Ito, F., Komatsubara, S., Ohata, H., and Yoshino, K., 2012, Roles of silica and lignin in horsetail (Equisetum hyemale), with special reference to mechanical properties, Journal of Applied Physics, v. 111(4), pp. 044703-1 to 0447703-6.
Yost, C.L. and Blinnikov, M.S., 2011, Locally diagnostic phytoliths of wild rice (Zizania palustris L.) from Minnesota, USA: Comparison to other wetland grasses and usefulness for archaeobotany and paleoecological reconstructions, Journal of Archaeological Science, v. 38, pp. 1977–1991.